ACKNOWLEDGEMENTS

The author would like to acknowledge the report supervisor, Prof. Mal Turaga for his guidance in this project and Mr. Hagop Evrensel, the lab technician, for his assistance in this project.

TABLE OF CONTENTS

NOTATIONS

A	Surface area, sq. ft.; A_F refers to fin, A_i refers to inside pipe, A_o refers to total outside surface
a	Coefficient in Eq (10), Btu per lba; a_R evaluated at refrigerant temperature t_R; a_w evaluated at water film temperature t_w
A_N	Nozzle's area, sq.ft.
b	Coefficient in Eq (10), Btu per (lba) (F); b_R evaluated at refrigerant temperature t_R; b_w evaluated at mean water film temperature $t_{w,m}$
C_p	Specific heat at constant pressure of tube-side fluid, Btu per (lb.) ($^\circ$F)
$C_{p,a}$	Specific heat at constant pressure of moist air per unit mass of dry air, Btu per (lba) ($^\circ$F)
h	Ethalpy of moist air, Btu per lba; h_1 refers to entering air; h_2 refers to leaving air
$h_{c,o}$	Convection heat transfer coefficient for outside surface, Btu per (hr), (sq ft) ($^\circ$F)
$h_{d,o}$	Mass Transfer Coefficient for outside surface, lb_w per (hr) (sq.ft.) (lb_w per lba)
$h_{d,i}$	Deposit coefficient for inside surface Btu per (hr) (sq.ft) ($^\circ$F)
h_F	Fictitious enthalpy of moist air defined by Eq (12); Btu per lba; $h_{F,m}$ evaluated at mean fin temperature $t_{F,m}$; $h_{F,b}$ evaluated at temperature $t_{F,b}$ of fin base; $\Delta h_F = h - h_F$, etc.

$h_{f,w}$ Enthalpy of saturated liquid water at temperature t_w Btu per lb_w

$h_{g,t}$ Enthalpy of saturated water vapor at air-dry bulb temperature, Btu per lb_w

h_i Heat Transfer Coefficient for inside surface, Btu per (hr), (ft^2), (°F)

$h_{o,w}$ Heat Transfer Coefficient, Btu per (hr). (sq ft). (°F), defined by Eq (16)

h_s Enthalpy of saturated moist air, Btu per lb_a; $h_{s,p}$ evaluated at pipe temp t_p; $h_{s,R}$ evaluated at refrigerant temp t_R; $h_{s,w}$ evaluated at water film temp t_w

Δh_m Mean enthalpy difference for moist air, Btu per (lb a)

h_{a1} Enthalpy of dry air at DB temperature entering intake chamber, Btu per lb dry air

h_{a2} Enthalpy of dry air at DB temperature leaving mining chamber, Btu per lb dry air

h_{g1} Enthalpy of saturated vapor at DB temperature entering intake chamber, Btu per lb water vapor

h_{g2} Enthalpy of saturated vapor at DB temp leaving mixing chamber, Btu per lb dry air

h_1 Enthalpy of air water vapor mixture entering coil at test conditions Btu per (lba)

h_2 Enthalpy of air-water vapor mixture leaving coil Btu per (lba)

h_3 Enthalpy of air water vapor mixture entering intake chamber

h_4 Enthalpy of air water vapor mixture leaving mixing chamber

k	Thermal conductivity, Btu per (hr), (sq ft), (°F) per ft; k_F refers to fin material; k_p refers to pipe material
L	Length, ft
Le	$h_{c,o}/h_{D,o}C_{p,a}$, dimensionless
m	Mass rate of flow of fluid inside outside of tubes, lb per hr
m_a	Mass rate of flow of dry air, lb_a per hr
P	$\sqrt{h_{c,o}/Ky}$ for dry fins, ft; $\sqrt{h_{o,w}/k_F\, y_F}$ for net fins, ft^{-1}
P_b	Barometric pressure, in hg abs
ΔP_N	Static pressure difference across nozzle or velocity pressure at nozzle exit, in of water
P_N	Static pressure at nozzle throat (or nozzle exit), converted to in Hg gauge
q	Rate of heat Transfer, Btu per hr; q_f refers to heat conduction in fins
q_{ta}	Total air side cooling and dehumidifying capacity, Btu
q_{sa}	Sensible air side cooling capacity by test, Btu
q_{tz}	Total fluid side heat capacity, Btu
q_t	Average total cooling capacity, Btu
q_s	Average sensible cooling capacity, Btu
t	Temperature of fluid outside of tubes, °F; t_1, refers to entering fluid; t_2 refers to leaving fluid
t_F	Temperature of fin, °F; $t_{F,B}$ refers to hose of fin; $t_{F,m}$ refers to mean fin temp; $\Delta t_F = t_F - t$, etc.
t_f	Temperature of fluid inside of tubes, °F
t_p	Temperature of pipe or tube; °F; $t_{p,i}$ refers to inside surface

t_R	Refrigerant temperature, °F
t_s	Temperature of saturated moist air, °F
t_w	Temperature of water film, °F; $t_{w,m}$ refers to mean value
Δt_m	Mean temp difference between fluids, °F
t_1	Air dry bulb temperature, entering coil at test condition
t_3	DB temperature, entering intake chamber, °F
t_4	DB temperature leaving mining chamber, °F
t'_4	Wet bulb temperature leaving mining chamber, °F
t_5	Average DB temp surrounding air intake and mining chamber, °F
U_o	Overall heat transfer coefficient, Btu per (hr).(ft^2).(°F)
$U_{o,w}$	Overall heat transfer coefficient for heat exchangers with wet fins, Btu per (hr).(sq ft).(Btu per lba)
V_a	Standard air face velocity, f.p.m.
V_N	Specific volume of air water vapor mixture at DB entering nozzle and humidity ratio of mixture entering nozzle, cu ft mixture per lb dry air
W_1	Entering humidity ratio; lb water vapor per lb dry air
W_2	Leaving humidity ratio, lb water vapor per lb dry air
W_a	Dry air flow rate, lb dry air per min
W_N	Humidity ratio of air water mixture entering nozzle
ϕ_w	Fin efficiency for wet fins defined by Eq (19), dimensionless

NOTATIONS FOR COMPUTER INPUT DATA

ASHRAE STD	FORTRAN PROGRAM	DESCRIPTION
T_3	T3	DB ENT. INTAKE CHAMBER, °F
T'_3	TP3	WB ENT. INTAKE CHAMBER, °F
T_4	TY	DB OUT. MIXING CHAMBER, °F
T'_4	TP4	WB OUT. MIXING CHAMBER, °F
T_5	T5	AVG. DB AROUND TEST CHAMBER, °F
T_A	TA	AMB. SURROUND REFRIG. COND.
T_N	TN	DB ENT. AIR NOZZLE(S), °F
T_{W1}	TW1	ENT. WATER (FLUID) TEMP. (CONDENSER), °F
T_{W2}	TW2	LEAVING WATER (FLUID) TEMP. (CONDENSER)
T'_2	TPR2	SUPER HEATED REFRIG. OUT SUCT. HDR., °F
H_{C1}	HC1	ENTHALPY OF REFRIG. ENT. COND., BTU/LB
H_{C2}	HC2	ENTHALPY OF REFRIG. OUT. COND., BTU/LB
H_{R1}	HR1	ENTHALPY OF REFRIG. ENT. COIL, BTU/LB
H_{R2}	HR2	ENTHALPY OF REFRIG. VAPOR OUT. COIL, BTU/LB
P_B	PB	BAROMETRIC PRESS DURING TEST, "HG ABS
P_N	PN	STATIC PRESS AT NOZZLE THROAT, "HG
P_{A1}	PA1	AIR STATIC AT TEST COIL INLET, "WG
P_{C1}	PC1	REF. VAPOR PRESS ENT. COND., PSIG
P_{R2}	PR2	REF. VAPOR PRESS OUT, COIL SUCT.HDR.PSIG
ΔP_A	DPA	AIR SIDE PRESS DROP THRU TEST COIL, "WG
ΔP_N	DPN	STATIC PRESS DIFF. ACROSS NOZZLES, "WG
ΔP_R	DPR	REFRIG. PRESS DROP THRU COIL & HDR., PSI
ΔP_{RC}	DPRC	REFRIG. PRESS DROP THRU COIL CIRCUIT, PSI

ASHRAE STD	FORTRAN PROGRAM	DESCRIPTION
C_N	CN	AIR NOZZLE COEFFICIENT
A_N	AN	AIR NOZZLE(S) AREA, SQ.FT.
A_F	AF	TEST COIL FACE AREA, SQ.FT.
K_C	KC	COND. INSULATION COEFFICIENT, BTU/(HR)^o(F)
K_{24}	K24	AIR MIXING CHAMBER HEAT LEAK, BTU/(HR)^o(F)
K_{31}	K31	AIR INTAKE CHAMBER HEAT LEAK, BTU/(HR)^o(F)
M	M	WEIGHT OF WATER (FLUID) COLLECTED, LBS
Z	Z	TIME REQ'D TO COLLECT WATER (FLUID), MIN.
W_{RF}	WRF	REFRIG. FLOW THRU FLOW METER, LBS/HR
	RT	REFRIG. TYPE NUMBER

NOTATIONS FOR COMPUTER OUTPUT DATA

W_1	W1	ENT. HUMIDITY RATIO, #WV/LB DA
W_2	W2	LEAVING HUMIDITY RATIO, #WV/LB DA
V_N	VN	SPEC. VOL. OF AIR VAPOR MIX AT STD Pg, CU.FT./LB.DA
W_A	WA	DRY AIR FLOW RATE, #DA/MIN
V_A	VA	STD. AIR FACE VEL. FT/MIN.
T_1	T1	DB ENT. COIL, °F
H_1	H1	ENTHALPY OF AIR ENTERING COIL, BTU/LB DA
T_2	T2	DB LEAVING COIL, °F
H_2	H2	ENTHALPY OF AIR LEAVING COIL, BTU/LB DA
Q_{TA}	QTA	TOTAL AIR SIDE HEAT CAPACITY, BTU/HR
Q_{SA}	QSA	SENSIBLE AIR SIDE HEAT CAPACITY, BTU/HR
Q_{TZ}	QTZ	TOTAL FLUID SIDE HEAT CAPACITY, BTU/HR
Q_T	QT	AVG. TOTAL HEAT CAPACITY, BTU/HR
Q_S	QS	AVG. SENSIBLE HEAT CAPACITY, BTU/HR
	HBT	HEAT BALANCE, TOTAL, %
ΔP_{st}	HBS	HEAT BALANCE, SENSIBLE, %
PST	DPS	STD. AIR PRESS DROP, in. of water
P_{R1}	PR1	ABS. REFRIG. PRESS AT COIL INLET, PSIA
P_{RC2}	PRC2	ABS. REFRIG. PRESS OUT COIL CIRCUIT, PSIA
P_{RH}	DPRH	REFRIG. PRESS DROP ACROSS SUCT. HDR., PSI
T_{R1}	TR1	SAT. REFRIG. AT COIL INLET, °F
T_{R2}	TR2	SAT. REFRIG. AT COIL OUTLET, °F
T_{R2}	TRSH2	REFRIG. VAPOR S.H. AT COIL OUT

CHAPTER 1

INTRODUCTION

INTRODUCTION

Air cooling and de-humidifying coils are used extensively for comfort as well as process applications in the air conditioning and refrigeration industry. The design criteria for most of these heat exchangers were developed at a time when the energy was cheap and abundent. Even though the coil itself does not 'consume' energy, its heat transfer performance plays a major role in the overall energy consumption of the air conditioning system in which it operates. The current energy crisis and soaring energy costs provide a strong incentive to improve the performance of these coils.

Air conditioning systems seldom operate at full load (3), and therefore, the performance evaluation of its components at part loads, is particularly important for an accurate assessment of energy consumption over the full range of system operation.

The peak load performance of cooling coils is generally determined by the manufacturers within a reasonable degree of accuracy. However, the part load performance evaluation requires much more sophisticated methods using special purpose test facilities such as the one at the Centre for Building Studies of Concordia University.

The major objective of this report is to present the experimental performance evaluation of a 10 ton direct expansion air cooling and

de-humidifying coil. This work is part of an overall research programme for the development of a Computer Assisted Direct Expansion Coil Design Programme in progress at Concordia University.

The author's contribution is mainly in the area of performing some of the measurements in the experimental work, literary search and the uncertainty analysis of the measurements for the test. The design of the test facility and the experimental work is performed by others (27), (30) and (33).

A brief literature survey of the existing information is presented in Chapter 2. Descriptions of the test facility, instrumentation and measurement system used, test procedures and the analysis of the results are presented in Chapters 4, 5 and 7.

CHAPTER 2

LITERATURE SURVEY

LITERATURE SURVEY

Extended surface coils used for cooling and de-humidifying air present complex problems due to many variables which affect their heat transfer performance. In air conditioning applications, the problem of designing coils in which the surface temperature is wholly or partly lower than the dew point of the incoming air is commonly encountered. In this situation, the moisture contained in the air is partly condensed, and this condensate transfers a certain amount of heat (latent heat) over and above that quantity of heat (sensible heat) which is transmitted when no condensation takes place. In other words, when a coil causes de-humidification to take place, the water vapor in the air, which exists in the form of super-heated steam, must be cooled and condensed by the cold surface. The vapor can reach the surface of the coil only by travelling through an air film that exists on the coil surface. This process occurs by diffusion and convection. When the vapor reaches the cold surface, it condenses and releases its latent heat. Simultaneously, the surrounding air is cooled sensibly.

The Heating Ventilating Air Conditioning Guide (1952) recommended a method of designing air coolers which had first been published by Tuve and Seigel in A.S.H.V.E. Transactions (4). This method has been subsequently described by Seigel in 1945, (5). In the introduction to their paper, Tuve and Seigel made a survey in which they mentioned the

advantages and the drawbacks of six other methods of coil design. In the discussion concluding their papers, several authors indicated that Tuve's and Seigel's method, which is called "the humidity method", is based on some simplified reasonings, which can, in certain cases lead to questionable results.

Another method, which seems to be more accurate from a theoretical point of view, but is rather intricate, has been described by Goodman in 1939, (6). The application of this method is confined to the design of air coolers, and presupposes that the difference between the surface temperature of the cold fluid is comprised within a limited range. Furthermore, this method includes an approximate analytical calculation of the dry-bulb temperature of the air at the outlet of the heat exchanger. For example, in his analysis, Goodman does not consider the effect of refrigerant oil film on the inside of the tube walls or the superheating of the refrigerant in the coil. Also, the conductivity of the metal walls and fins is assumed to be infinite. The great difference between the heat transmission of the air and refrigerant films and the heat transmission of the metal walls and fins was used by Goodman to justify the omission of these factors. This assumption does not permit any consideration of the efficiencies of the fins under wet and dry conditions. In fact, he, like the other authors, who have studied this problem (prior to 1940), has not taken into account of the fact that thermal efficiency of the fins is dependent on whether the surfaces are moist or dry.

Gosta Brown (7) has described "Theory of Moist Air Heat Exchangers" which has been published in Stockholm as a Transaction of the Royal Institute of Technology in 1954, (8).

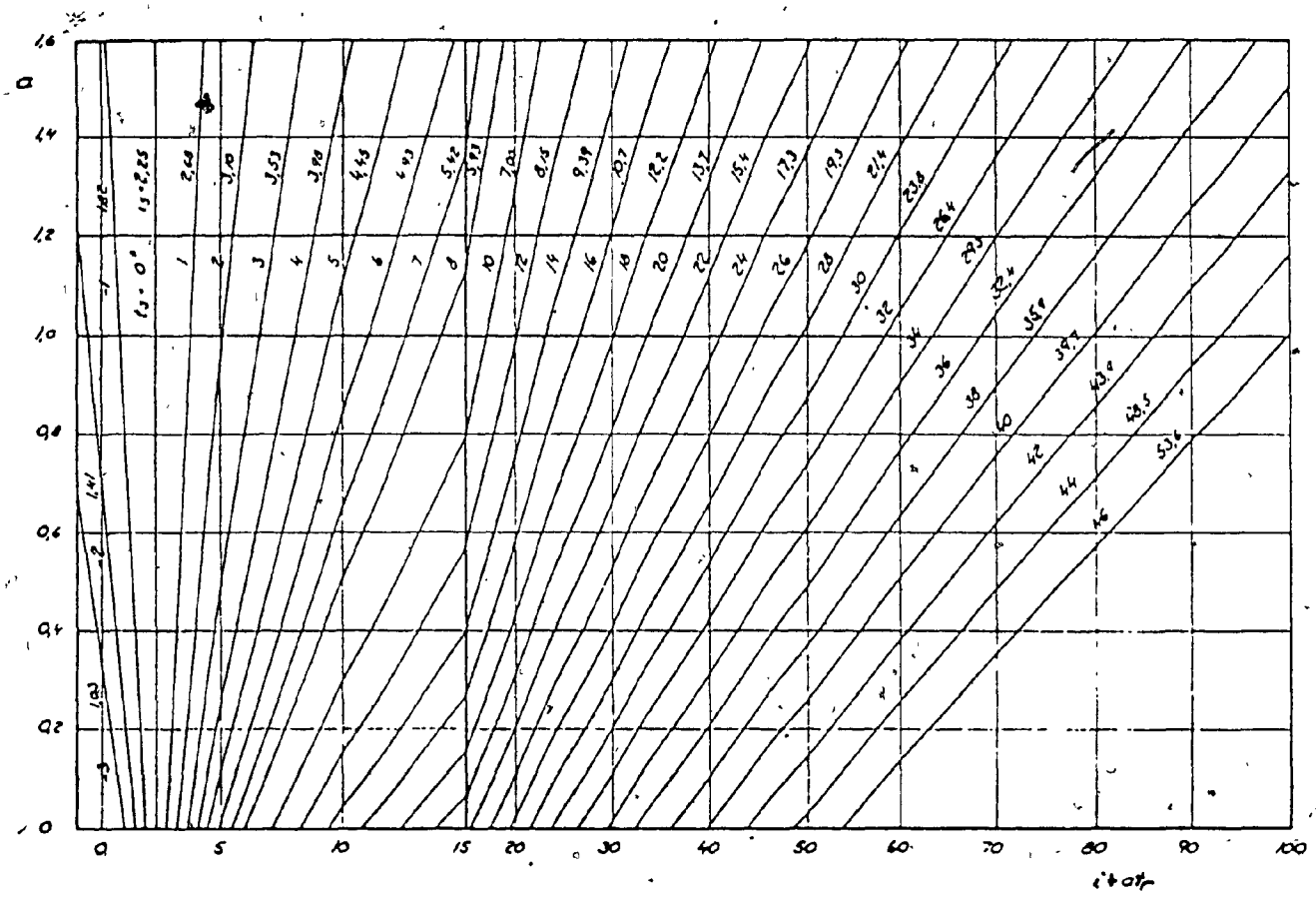

Figure 1. Graph for determining the temperature at the enthalpy of air at a moist surface

In this analysis, Brown suggested a method for the calculation of the wet surface temperature in a moist heat exchanger. For this purpose, he first calculates the 'true' coefficient of heat transfer surfaces (as a function of air velocity in dry air heat exchanger) and then calculates the thermal efficiency of fins in moist air heat exchangers. He uses a linear graphical relationship between i_s and t_s as shown in figure where

i_s - the enthalpy of saturated air at a moist surface, K cal/kg dry air

f_s - temperature of a moist, ^oC

The parameter 'a', (in the vertical axis) is defined as :

$$a = \frac{Cp}{\alpha_1} \quad \frac{Fr}{F} \quad \frac{1}{1/\alpha_1 + M}$$

where

Cp = the specific heat of moist air, K cal/^oC kg of dry air

= the coefficient of heat transfer between the air and the moist surface, K cal/$m^2 h\,^oC$

F = the area of the moist surface, m^2

Fr = the area of the heat exchanger surface on the refrigerant side, m^2

M = the thermal resistance of the heat exchanger wall and of the scale deposits (if any), m^2, ^{o}(F) per Btu

(This method of representation offers the advantage that the family of curves consisting of straight lines, but the relations between t_s and i_s is not linear.) Brown's method is more accurate from a theoretical point

of view, compared to the methods described so far. Furthermore, this method could be adapted for practical applications. The relationship between 't_s' and 'i_s' is expressed through a family of curves in this method. However, the direct relationship between the two variables is not always linear, which could result in some error.

J.L. Threlkeld, (9) in his analysis of heat transfer in wet-surface cooling coils, considers the variation of wetness of the cold surface in contact with a moving stream of a moist air more thoroughly. This method has been discussed more in detail in the next chapter. Threlkeld's theoretical work is verified experimentally by Myers, (10). Myers made a comprehensive study comparing the coefficient $h_{c,o}$ (convection heat transfer coefficient for outside surface) for a wet-surface cooling coil to that for the same coil operated without dehumidifaction. Myers experimental coil was very similar to surface (1) of Table 1 and Figure 2. Figure 3 shows Myers correlations for heat transfer to the external surface both for dry surface (cooling without dehumidification) and for wet-surface operation (cooling and dehumidification).

* TABLE 1

DIMENSIONAL DATA FOR TWO PLATE-FIN-AND-TUBE SURFACE ARRANGEMENTS

Data	Surface I	Surface II
Dimensions (*See sketch with Fig.* 12.15.)		
A, tube outside diameter, in.	0.402	0.676
B, tube spacing across face, in.	1.00	1.50
C, tube spacing between rows, in.	0.866	1.75
D, spacing of fins, center to center, in.	0.125	0.129
E, thickness of aluminum fins, in.	0.013	0.016
Flow passage hydraulic diameter, $4r_h$, ft	0.01192	0.01268
Area Data		
$A_{o,t}$, sq ft external surface/(sq ft face area) (row)	12.92	22.86
$A_o/A_{p,t}$, sq ft external surface/sq ft internal surface	12.27	19.31
A_c, sq ft net flow area/sq ft face area	0.534	0.497
A_F/A_o, sq ft fin surface/sq ft external surface	0.839	0.905

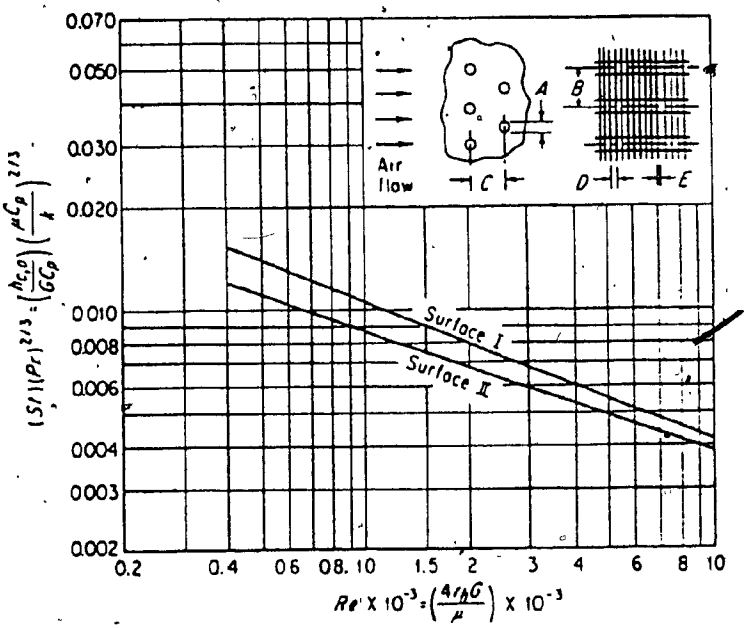

*Fig. 2 - Correlated external surface heat transfer data for surface of Table 1.

*Extracted from (9)

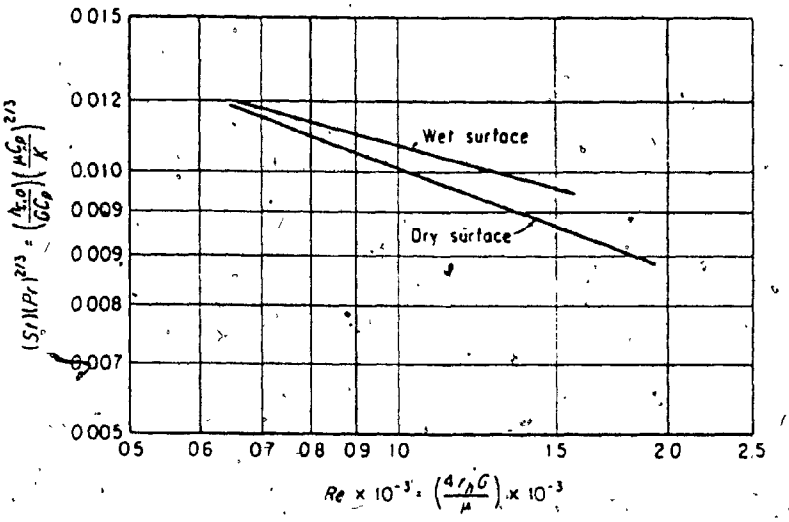

*Fig. 3 - Dry surface and wet-surface correlation for the external surface of a finned tube cooling coil.

* Extracted from (9)

CHAPTER 3

THE THEORETICAL ANALYSIS OF THE PERFORMANCE OF DIRECT EXPANSION COOLING COILS

3.1 THEORY OF HEAT TRANSFER IN WET-SURFACE COOLING COILS:

In this chapter an analysis of the fundamental concepts of refrigerant to air heat transfer for ideal counter flow situation, is presented.

Heat transfer through a moist surface takes place partly by conduction, convection and radiation, and partly by evaporation or condensation. Evaporation occurs when the surface temperature is higher than the dew point of the air, while condensation takes place when the air stream temperature drops below the dew point. As has already been point out, with de-humidification, the air side surface is wetted (by the condensate water or frost). Besides transfer of sensible heat, there is a transfer of latent heat because of condensation. Figure 4 shows schematically a cold surface in contact with a moving stream of moist air. A moving film of water is formed on the surface by condensation of moisture from the air steam. There is a boundary layer of air next to the water surface. In this layer, it is assumed that air temperature, air humidity ratio, and air velocity vary in a plane perpendicular to bulk motion of the air.

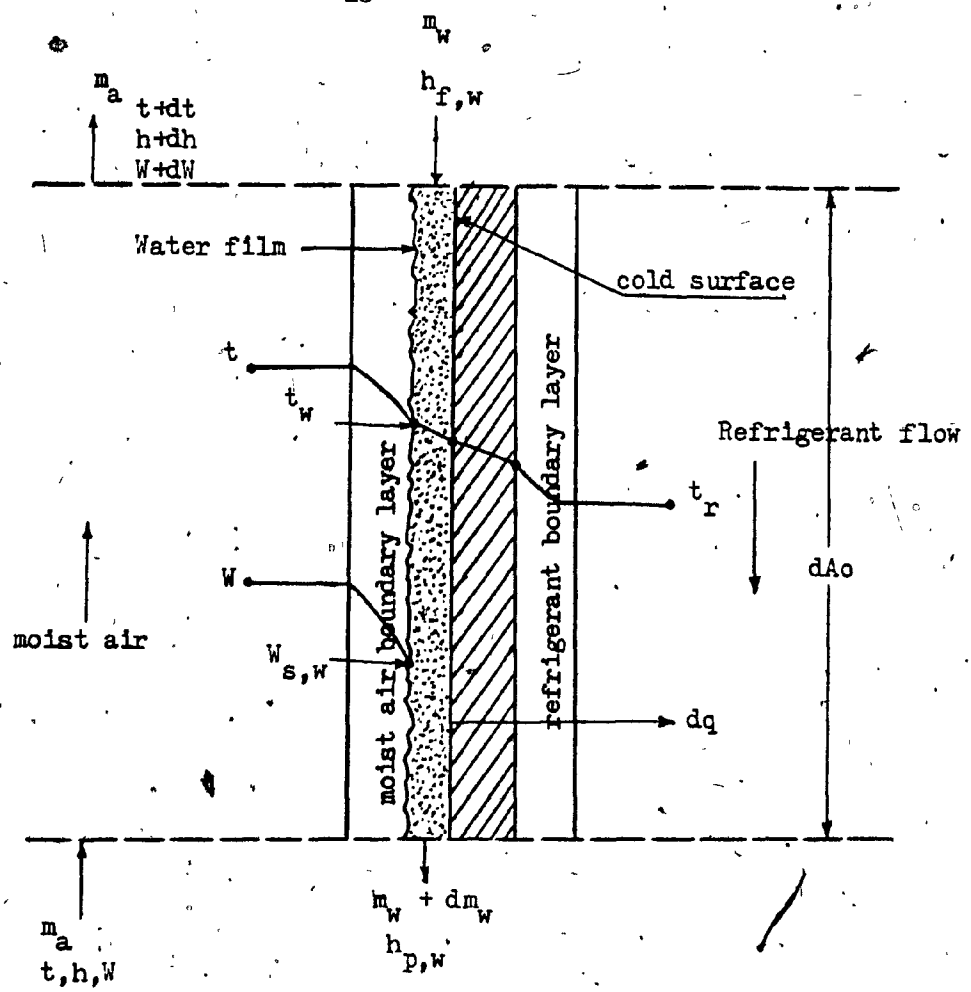

Figure 4 schematic cooling and dehumidifying of moist air

Immediately at the air-water interface, next to the water film, it is assumed that the air is saturated at the water surface temperature t_w. For the differential surface area in Fig. 4, the heat balance equation can be written as follows:

$$-m_a\, dh = dq - m_a\, dw\, h_{f,w} \qquad (1)$$

$$dq = h_{c,o}\, dA_o (t-t_w) + h_{D,o}\, dA_o (W-W_{s,w})(h_{g,t}-h_{f,w}) \qquad (2)$$

$$-m_a\, dw = h_{D,o}\, dA_o (W-W_{s,w}) \qquad (3)$$

Using the relation $Le = h_{c,o}/h_{D,o}\, C_{p,a}$, Eq(2) may be written as :

$$dq = h_{c,o}\, dA_o / C_{p,a} \left[C_{p,a}\,(t-t_w) + (W-W_{s,w})(h_{f,t} - h_{f,w})/Le \right] \qquad (4)$$

or

$$dq = \frac{h_{c,o}\, dA_o}{C_{p,a}} \left[(h-h_{s,w}) + \frac{(W-W_{s,w})(h_{g,t} - h_{p,w} - 1061\ Le)}{Le} \right] \quad (5)$$

By Eq (1), (3) and (5), it may be shown that:

$$\frac{dh}{dw} = Le \frac{(h-h_{s,w})}{(W-W_{s,w})} + (h_{g,t} - 1061\ Le) \quad (6)$$

Eq (6) describes the process line on psychometric chart for the cooling and dehumidifying of moist air by a cold surface.

In eq (5), the latter grouping in the brackets is typically small compared to the term $(h-h_{s,w})$. For example, if the air state was 85°F, dry-bulb temperature, 70°F thermodynamic wet-bulb temperature, and 14.696 psia barometric pressure, and the water film temperature was 60°F, we would have

$$h-h_{s,w} = 7.51 \text{ Btu/lba}$$

$$(W-W_{s,w})(h_{g,t} - h_{f,w} - 1061\ Le) / Le = 0.142 \text{ Btu/lba}$$

Thus, eq (5) can be written in a simplified form as :

$$dq = h'_{c,o}\, dA_o / C_{p,a} \times (h - h_{s,w}) \quad (7)$$

3.2 The Efficiency of Wet-Surface Cooling Coil

In this section, the performance of a bar fin is presented when condensation occurs on its surface. Assuming that the heat conduction through the water film occurs in only the y direction, as shown in Fig. 5. For a unit length of the fin, we have

$$q_f = 2\, K_F\, Y_F \frac{dt_F}{dx} \quad (8)$$

where the subscript F refers to the metal fin. Also

$$dq_F = 2 \frac{Kw}{Yw} (t_w - t_F)\, dx \qquad (9)$$

where Kw and Yw are respectively the thermal conductivity and thickness of the water film. It's assumed that over a small gauge of temperature,

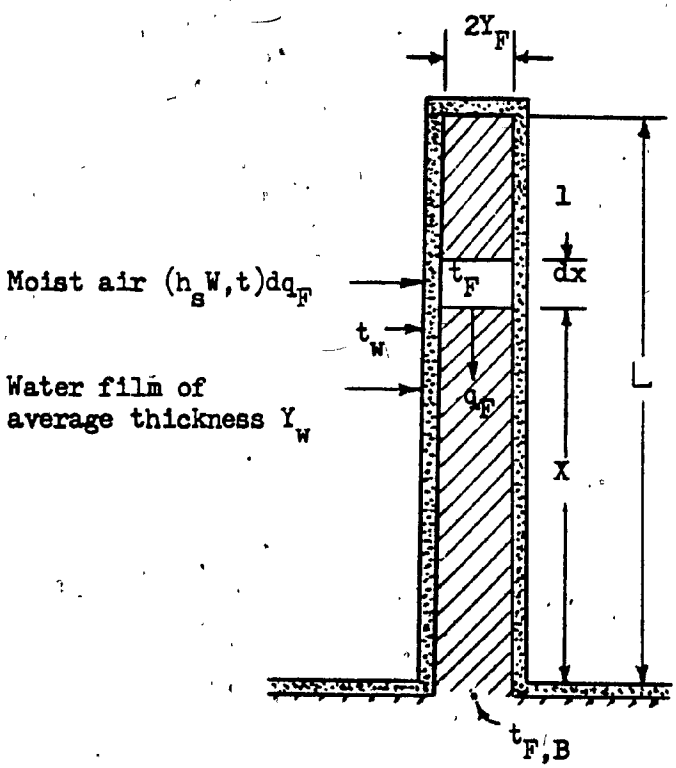

Figure 5 Schematic illustration of a bar fin wetted with moisture condensed from moist air.

the enthalpy of saturated air h_s, may be represented as :

$$h_s = a + bt_s \qquad (10)$$

By eqs (9) and (10),

$$dq_F = - \frac{2Kw}{bwYw} \left(h_{s,w} - q_w - b_w t_F\right) dx \qquad (11)$$

But the quantity $(a_w + b_w t)$ has the dimensions of moist air enthalpy, defining a fictitious air enthalpy h_F as

$$h_F = a_w + b_w t_F \qquad (12)$$

where the quantities a_w and b_w are evaluated at the surface temperature t_w. Thus,

$$dq_F = - \frac{2Kw}{b_w Yw} \left(h_{s,w} - h_F\right) dx \qquad (13)$$

By eq (7)

$$dq_F = - \frac{2h_{c,o}}{C_{p,a}} X \left(h - h_{s,w}\right) dx \qquad (14)$$

By eqs (14) and (13), we obtain

$$dq_F = - \frac{2h_{o,w}}{b_w} (h - h_F) dx = \frac{-2h_{o,w}}{b_w} h_F \, dx \qquad (15)$$

where $\Delta h_F = (h - h_F)$ and

$$h_{o,w} = \frac{1}{C_{p,a}/(b_w h_{c,o}) + Yw/Kw} \qquad (16)$$

By eqs (8) and (12), we have

$$q_F = \frac{2K_F Y_F}{b_w} \frac{dh_F}{dx} = - \frac{2 K_F Y_F}{b_w} \frac{\Delta h_F}{dx}$$

and thus

$$dq_F = -2 \frac{K_F Y_F}{b_w} \frac{d^2 \Delta h_F}{dx2} dx \qquad (17)$$

By eqs (15) and (17)

$$\frac{d^2 \Delta h_F}{dx2} = \frac{h_{o,w}}{K_F Y_F} \Delta h_F \qquad (18)$$

The boundary conditions for eq (18) are $\Delta h_F = \Delta h_{F,B}$ at $x = 0$ and $d\Delta h_F/dx = 0$ at $x = L$

The solution of eq (18) is the same as for dry finned tube heat exchanger. Furthermore, definitely the efficiency of the wet fin as

$$\phi_w = \frac{h - h_{F,w}}{h - h_{F,B}} = \frac{\Delta h_{F,w}}{\Delta h_{F,B}}$$

we find that

$$\phi_w = \frac{\tan h\, P\, L}{P\, L}$$

where $P = \sqrt{h_{o,w}/(K_F Y_F)}$

3.3 The Theoretical Analysis of Overall Heat Transfer Coefficient for a Wet Finned Tube Heat Exchanger for Cross-Flow Situation:

In this analysis, it is assumed that the thermal resistance of the tube wall is negligible, and that the tube has a uniform surface temperature t_p. It is also assumed that the fin and tube are covered by Thin Film of water having an average thickness Y_w.

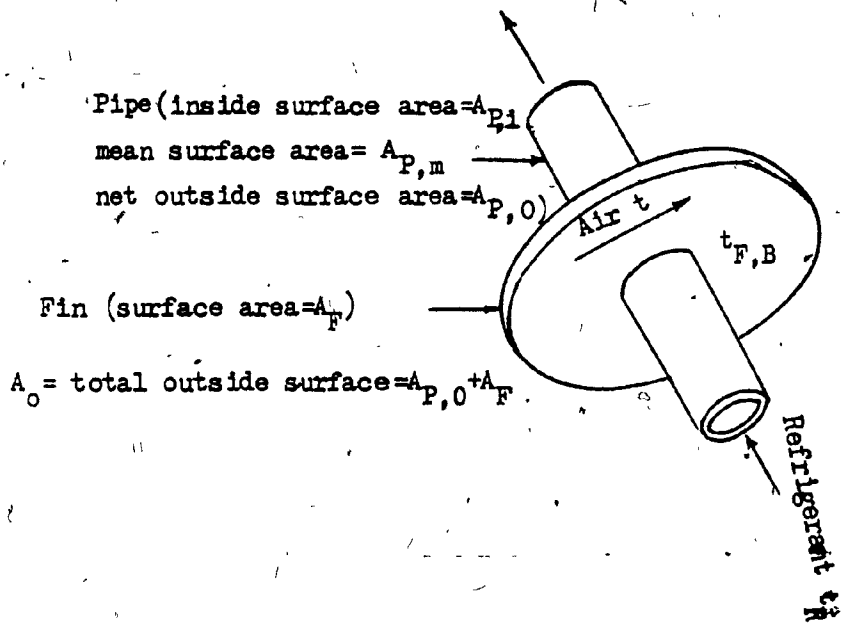

t_∞ = air temperature
$t_{F,B}$ = fin base temp
$t_{P,O}$ = pipe outer surface temperature = $t_{F,B}$
$t_{P,i}$ = pipe inner surface temperature
t_R = refrigerant temp
$t_{f,m}$ = mean fin temp.

Figure 6 Schematic Illustration for a finned tube heat exchanger.

As shown in Figure 6, the air passing over the surface has an enthalpy 'h', the local rate of heat transfer will be:

$$q = h_i \; A_{p,i} \; (t_p - t_r) \qquad (20)$$

By definition

$$b'_R = \frac{h_{s,p} - h_{s,r}}{t_p - t_r} \qquad (21)$$

where $h_{s,p}$ and $h_{s,r}$ are fictitious enthalpies of saturated moist air evaluated at the respective temperatures t_p and t_r. By eqs (20) and (21), it is obtained:

$$q = \frac{h_i \; A_{p,i}}{b'_r} \; (h_{s,p} - h_{s,r}) \qquad (22)$$

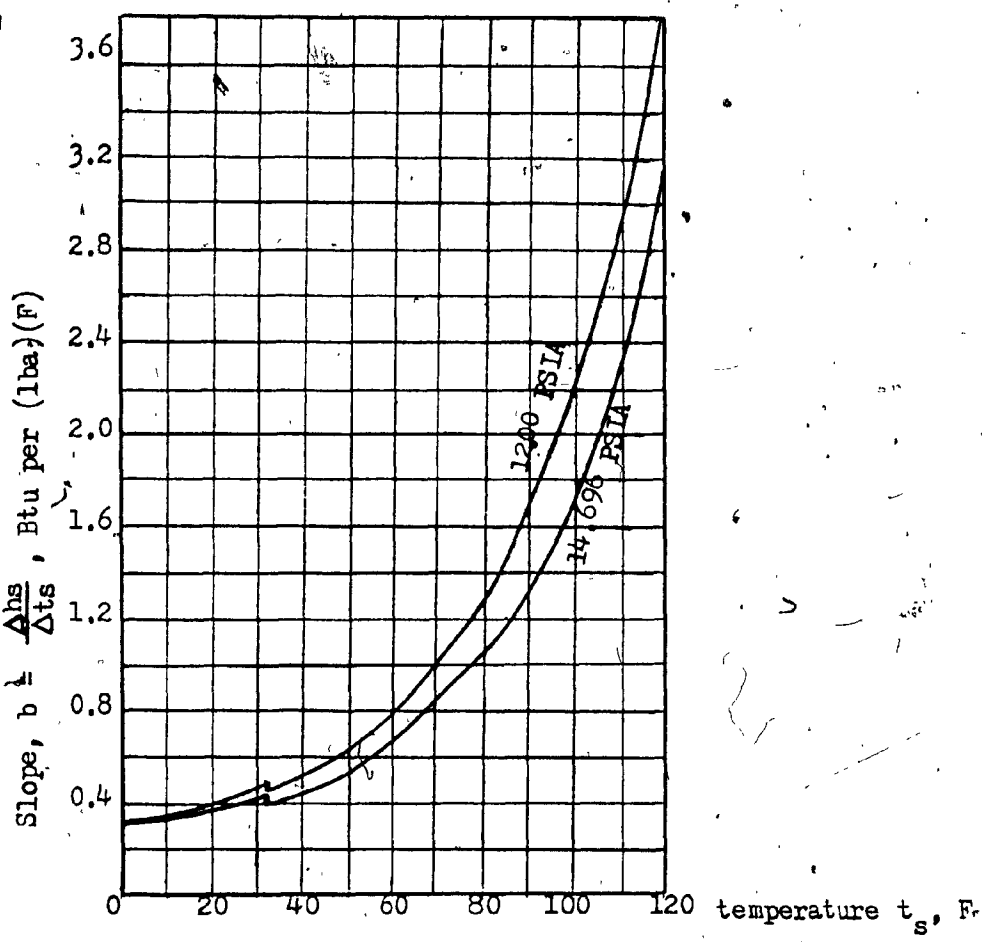

Fig. 7 , slope $ph_s/\Delta t_s$ for saturated air

By Eq (16), $h_{o,w}$ is known, thus

$$q = \frac{h_{o,w}}{b_{w,p}} A_{p,o} (h - h_{s,p}) + \frac{h_{o,w}}{b_{w,m}} A_F (h - h_{F,M}) \quad (23)$$

where $b_{w,p}$ is evaluated from Fig. 7 at the temperature of the surface of the water film on the tube and $b_{w,m}$ is evaluated at the mean surface temperature of the water film on the fin.

Making the approximations $b_{w,p} = b_{w,m}$ and $h_{s,p} = h_{F,B}$, with Eq (19) we have

$$q = \frac{h_{o,w}}{b_{w,m}} (A_{p,o} + \phi_w A_F) (h - h_{s,p}) \quad (24)$$

By definition of $U_{o,w}$ we may write

$$q = U_{o,w} A_o (h - h_{s,r}) \quad (25)$$

we may write by Eqs (24) and (25) that

$$U_{o,w} = \frac{1}{\frac{b'_r A_o}{A_{p,i} h_i} + \frac{b_{w,m} (1-\phi_w)}{h_{o,w} (A_{p,o} + \phi_u)} + \frac{b_{w,m}}{h_{o,w}}} \quad (26)$$

In order to calculate $U_{o,w}$ by above equation, we must first assume values of the mean water film surface temperature $t_{w,m}$ and the pipe temperature t_p. These assumptions allow initial approximations to be made for $b_{w,m}$ and b'_r respectively. After calculation of $U_{o,w}$, the validity of the assumptions must be verified. The procedure for this verification is as follows :

$$q = U_{o,w} A_o (h - h_{s,r}) \quad (27)$$

By Eqs (20) and (27), the pipe temperature t_p can be expressed as :

$$t_p = t_r + \frac{U_{o,w} A_o (h-h_{s,r})}{\phi h_i A_{p,i}} \qquad (28)$$

To establish a procedure for checking $t_{w,m}$, we begin by writing the relation

$$h-h_{F,m} = \phi_w (h-h_{s,p}) = \frac{b_{w,m} h_{c,o}}{h_{o,w} C_{p,a}} (h-h_{s,w,m}) \qquad (29)$$

By Eqs (22) and (27),

$$h-h_{s,p} = \left(1 - \frac{b'_r U_{o,w} A_o}{h_i A_{p,i}}\right)(h-h_{s,r}) \qquad (30)$$

Thus

$$h'_{s,w,m} = h - \frac{C_{p,u} h_{o,w} \phi_w}{b_{w,m} h_{c,o}} \left(1 - \frac{b'_r U_{o,w} A_o}{h_i A_{p,i}}\right)(h-h_{s,r}) \qquad (31)$$

Eq (31) allows determination of $t_{w,m}$ through calculation of the enthalpy of saturated air, $h_{s,w,m}$ at the same temperature.

3.4 Theory of Heat Transfer in Direct Expansion Coils

Most of the existing theoretical and experimental analysis related to heat transfer in cooling and dehumidifying coils, including those described so far in this chapter are performed using chilled water as refrigerant. In chilled water coils, the refrigerant does not go through those changes during the heat exchange process. That is, on the refrigerant side of the coil the heat transfer is basically sensible in nature.

A number of authors (12) to (25) performed experimental studies on heat transfer with boiling refrigerants. Most of their studies were conducted with constant heat flux on the tube surface using electrically heated water as heating medium. However, in actual situations, for air cooling and dehumidifying coils, the same level of uniformity of heat flux on the coil surface cannot be easily achieved. This is due to the fact that warm moist exhaust air moving at relatively high velocities (200 - 800 F.P.M.) over the coil surface

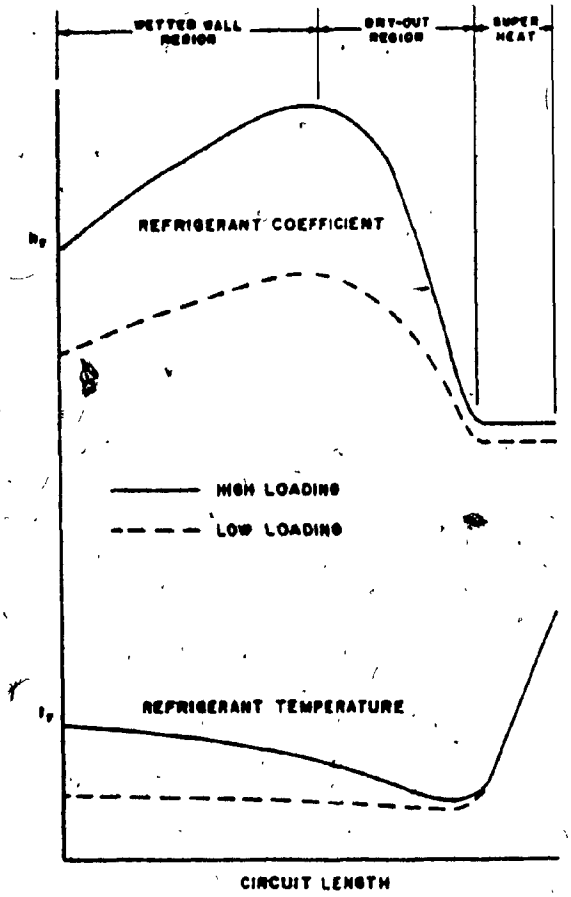

* *Fig. 8 Heat transfer coefficient and temperature vs circuit length*

* Extracted from (40)

provides the heat source. Therefore, to determine the heat transfer performance of the cooling coils, it is necessary to experimentally test coils of selected configurations under conditions as close to the actual working situation as possible. The test conditions for evaluating the heat transfer for such coils is described in ASHRAE standard 33-78 and ARI standard 410-72.

One of the few existing experimental studies on the performance of direct expansion coils is conducted by Rich and Chaddock (25) in 1970. Fig. 8 illustrates the heat transfer coefficients and temperature variations of a refrigerant as it moves through an evaporator tube.

In Fig. 8 two sets of curves are shown, one for high loading and the other for low loading on the coil. As shown in this figure, the heat transfer coefficient increases to a maximum and then decreases sharply, eventually reaching a value corresponding to that for pure gas flow in the 'superheat' section. The decrease in the heat transfer coefficient is due to the development of dry areas on the wall.

It is clear from Fig. 8 that an accurate calculation of the heat transfer in an evaporator can not be made using a single average value of the refrigerant coefficient. Ideally, a step-by-step calculation should be performed such that local variations in coefficient, refrigerant temperature, air enthalpy, and surface temperature are accounted for. Such a procedure, however would be complex and time consuming. As a first approximation, therefore, in this method the coil is divided into two

sections; an evaporation section and a superheat section, with average coefficient determined for each. Coil capacity is then calculated as follows :

$$q = \left\{ \frac{F_s S_o \; t_m}{R_r + R_m} \right\}_{evap.} + \left\{ \frac{F_s S_o \; t_m}{R_r + R_m} \right\}_{sup.}$$

where

S_o = external surface area (prime plus finned)

t_m = mean temperature difference between the refrigerant and the melted coil surface

R_r = thermal resistance of heat transfer between the refrigerant and the inside surface of the tube wall per unit of external surface area

R_m = thermal resistance of the fin and tube material per unit of external surface area

F_s = a safety factor specified by the designer

CHAPTER 4

PERFORMANCE EVALUATION OF DIRECT EXPANSION COOLING COIL

4.1 Performance Evaluation of the 10 Ton, 4 Row Direct Expansion Air Cooling and Dehumidifying Coil:

In this section the construction details of the test chamber and air side performance data are described. The major equipment and test coil specifications are shown in Appendix 2. The objective of these tests is to determine:

1. Air side and refrigerant side heat transfer data
2. Air side and refrigerant side pressure drop data at various coil air face velocities.

A number of other similar coils with a variable fin and tube spacing with the same tube diameter and surface area will be tested to generate a data bank which will eventually be used to develop a computer assisted coil selection and design programs.

4.2 Description of the Heat Exchangers Testing Apparatus

The test chamber consists of a closed loop air circulation system driven by a variable volume air handling unit. As shown in Fig. 9, air at a pre-determined rate is passed through a flow adjustment device, where the velocity is kept at a desired value before approaching the test coil. The flow adjustment device helps to maintain a constant approach velocity profile as required by A.S.H.R.A.E. standards (1). The incoming air is cooled and dehumidified by the test coil (item 9). The "cool" air then is passed through a nozzle section, item 10, where the air volume flow rate is measured. To keep the intake conditions constant at item 9, air is then

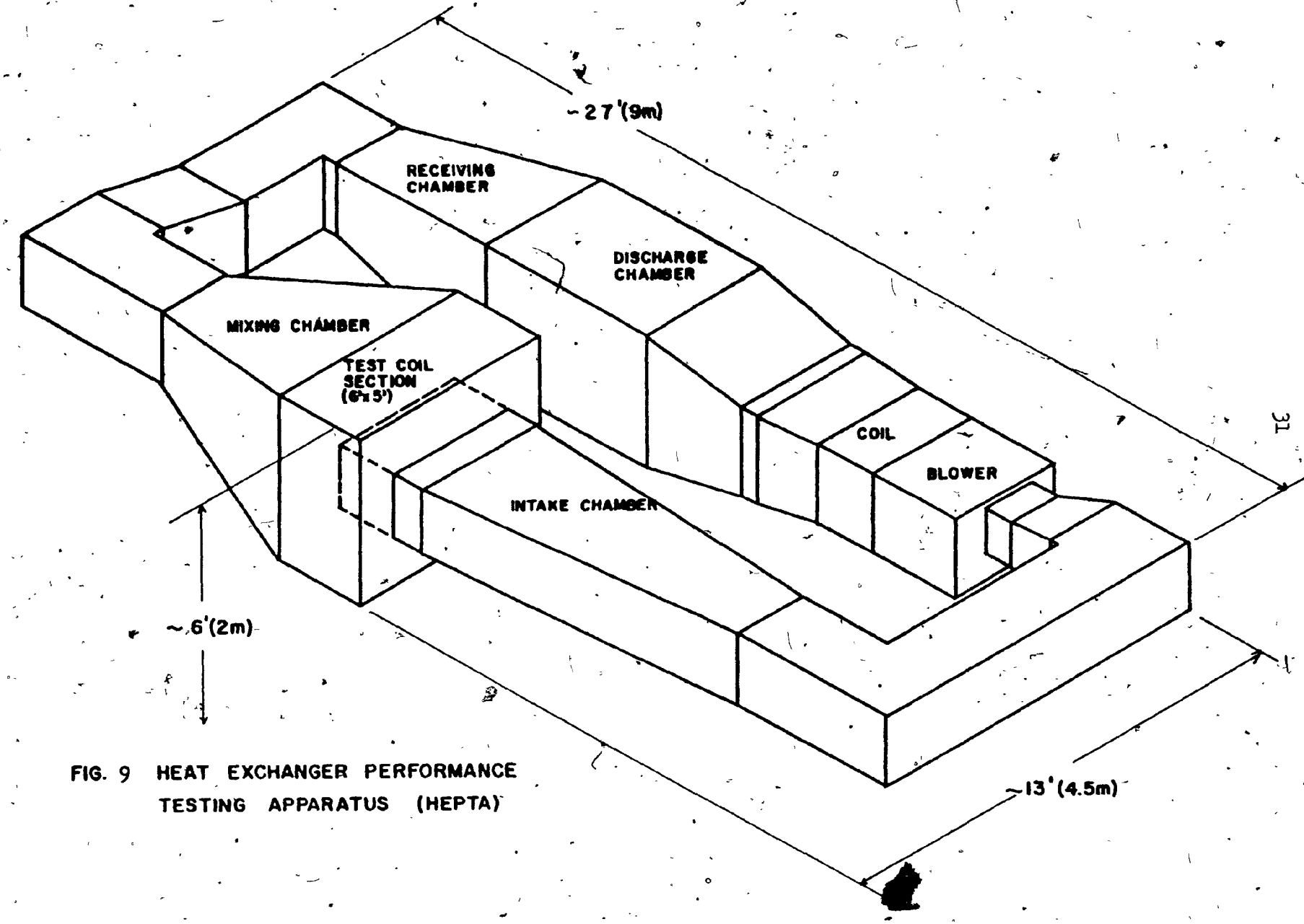

FIG. 9 HEAT EXCHANGER PERFORMANCE TESTING APPARATUS (HEPTA)

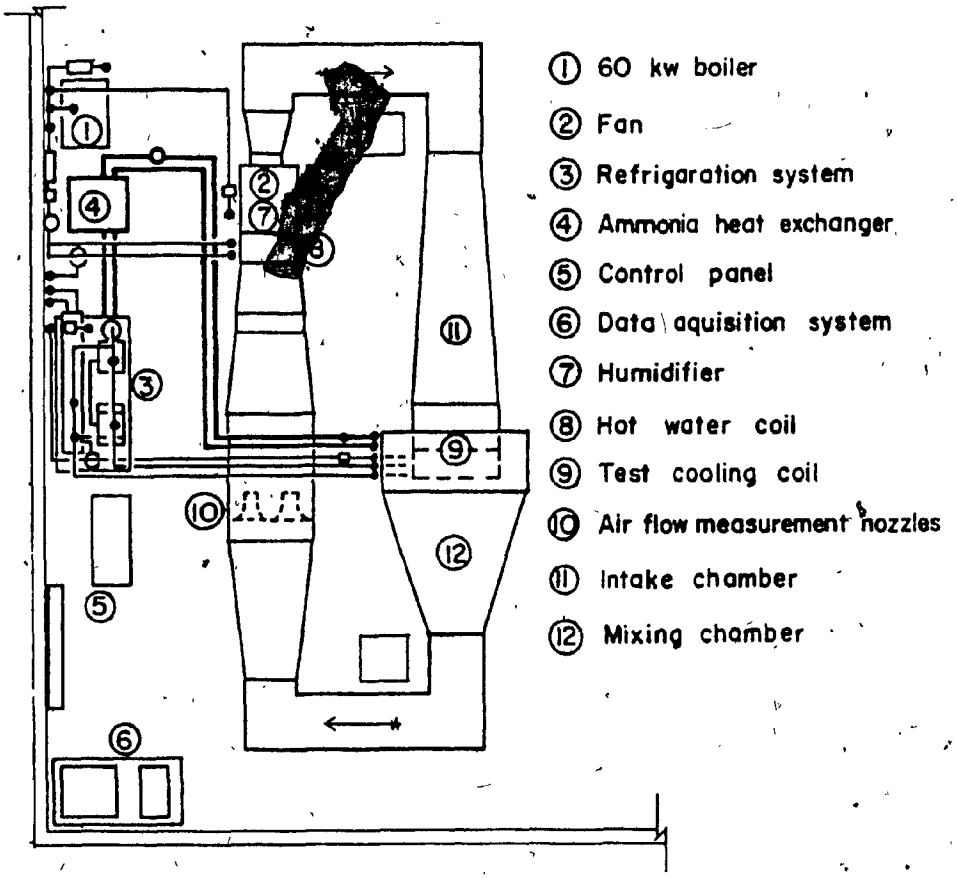

FIGURE 10. Equipment layout for heat exchanger performance testing apparatus (HEPTA).

heated in the hot water heating coil (item 8), humidified by a steam-jet humidifier (item 7), and is recirculated in the system by the variable volume fan (item 2). Air thermodynamic conditions are measured at both sides of the test coil (item 9).

A 60 k.w. electric steam boiler (item 1, Fig.10) provides the required hot water for heating and steam for humidification. The hot water is generated in a steam-to-water heat exchanger and is circulated to the heating coil through a circulating pump controlled thermostatically by a 3-way valve as shown in Fig. 11 . A steam jet humidifier (item 7, Fig.10 and Fig.12 controlled by a humidostat, provides the dry steam for humidification.

The main advantage of the closed-loop air circulation system over the standard open-loop system is the ease of control of incoming air psychometric conditions since this air is not subjected to fluctuations of the surrounding room temperature and humidity, (which is the case in standard open-loop systems).

Even though round ducts are recommended by the standards for these tests, a rectangular duct was used because of its wide application in commercial installations;this makes simulation of the actual working conditions more realistic. To minimize pressure losses in the loop and to provide a smooth velocity profile, "airo-foil" type turning vanes are used at the bends. The internal surfaces of the intake and mixing chambers are insulated with one inch thick foil protected rigid polyurethane insulation

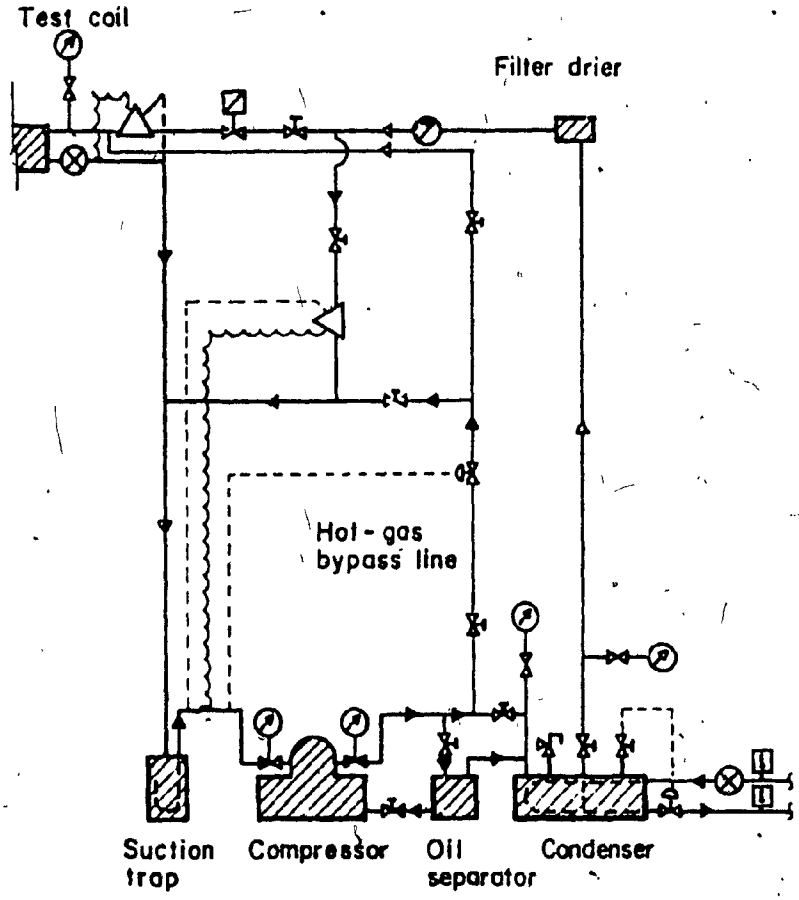

Figure 11 Refrigeration system flow diagram.

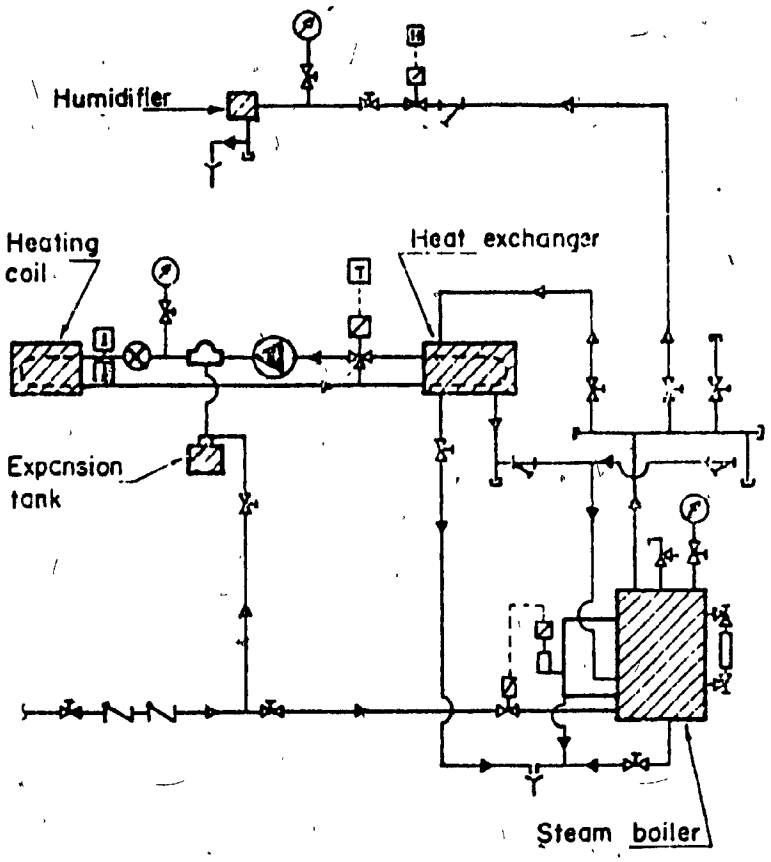

Figure.12 Heating and humidifying system flow diagram.

with an "K"-value of 6.54 Btu in/ft^{2}hr $^\circ$F (941.76 W mm/m^2 $^\circ$C) per $^\circ$F. The foil also provides a smooth surface for air flow.

The test chamber is made up of a number of aligned, bolted, sections with rubber gaskets and sealed for air tightness. These sections can be interchanged with other appropriate sections to accommodate other types of heat exchangers.

4.3 "Air Side" Performance Data for the Test Chamber

In any heat exchanger performance test where air is one of the mediums in the heat exchange process, it is essential to develop a full understanding of the performance of the air handling equipment as well as the "air side" of the system. " Air side" system components include all the components of the system through which the air under study passes. It is necessary to determine the various test velocities, corresponding air volumes and static pressures at critical points in the system to be able to determine the heat transfer rates accurately.

In this test chamber, air flow rates and air static pressures can be varied both by adjustment of the fan exit damper and by closing one or more of the four flow measurement nozzles.

The "air side" performance is determined experimentally in this chamber and results are shown in the following graphs:

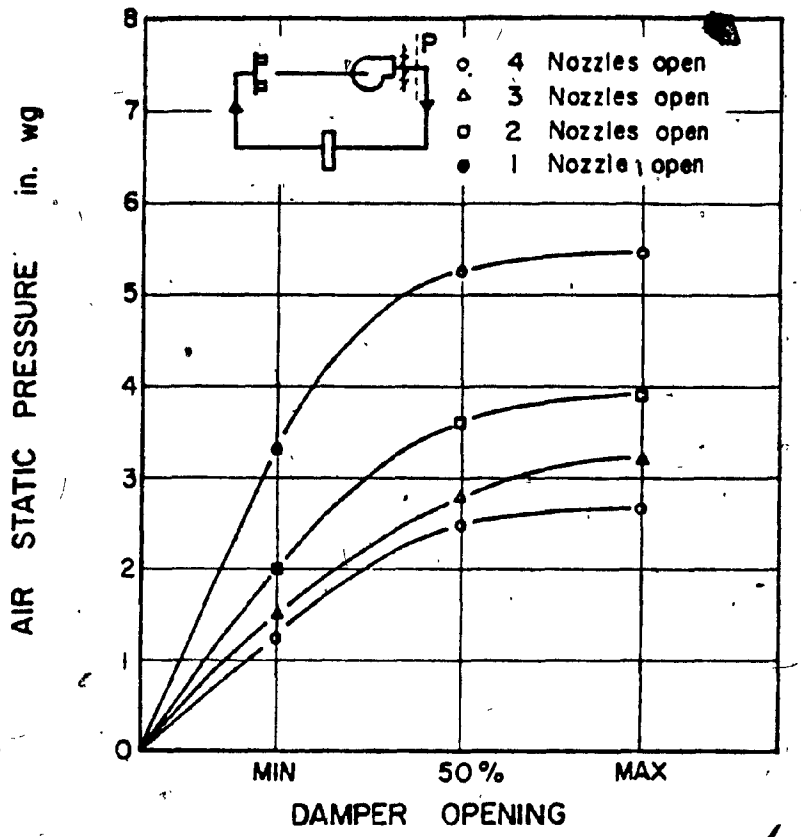

Figure 13 Air static pressures at the fan exit for various damper positions.

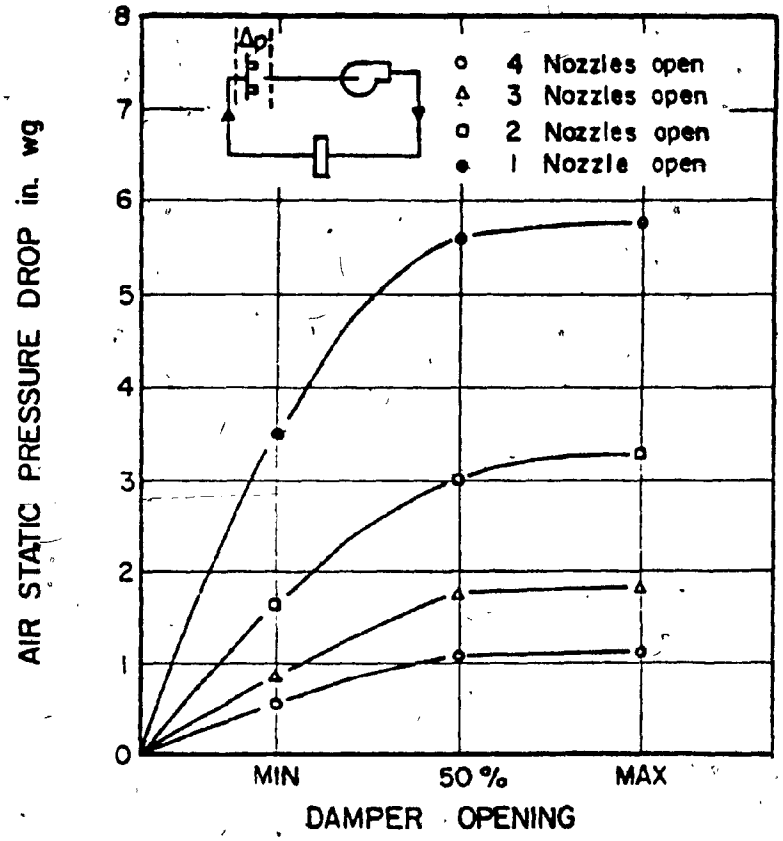

Figure 14 Air static pressure drops across the flow measurment nozzles for various damper openings.

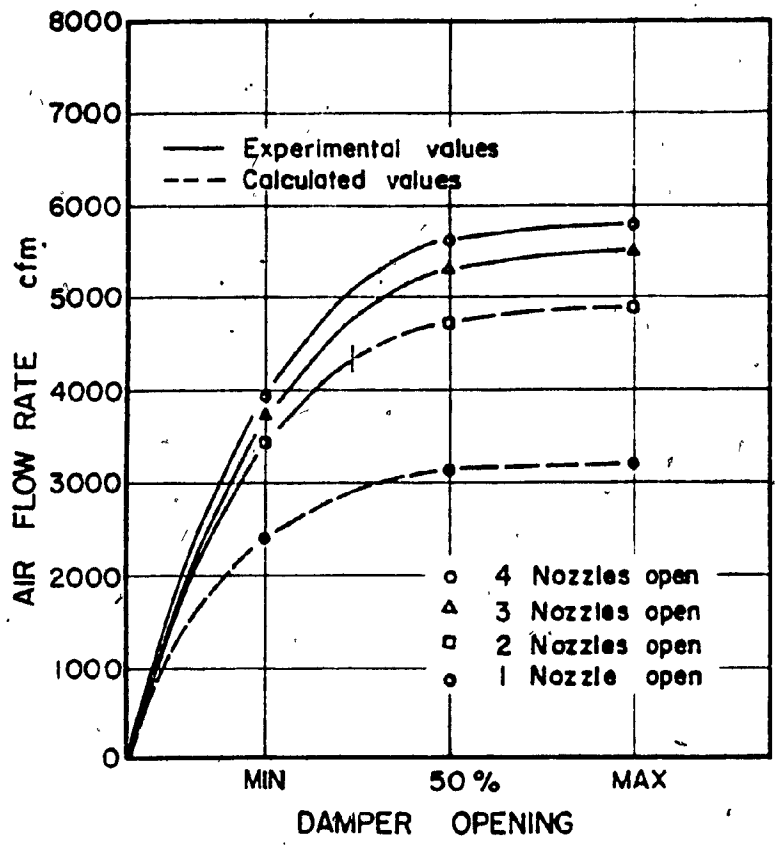

Figure 15 Fan air flow rates calculated from air static pressure drops across the flow measurement nozzles.

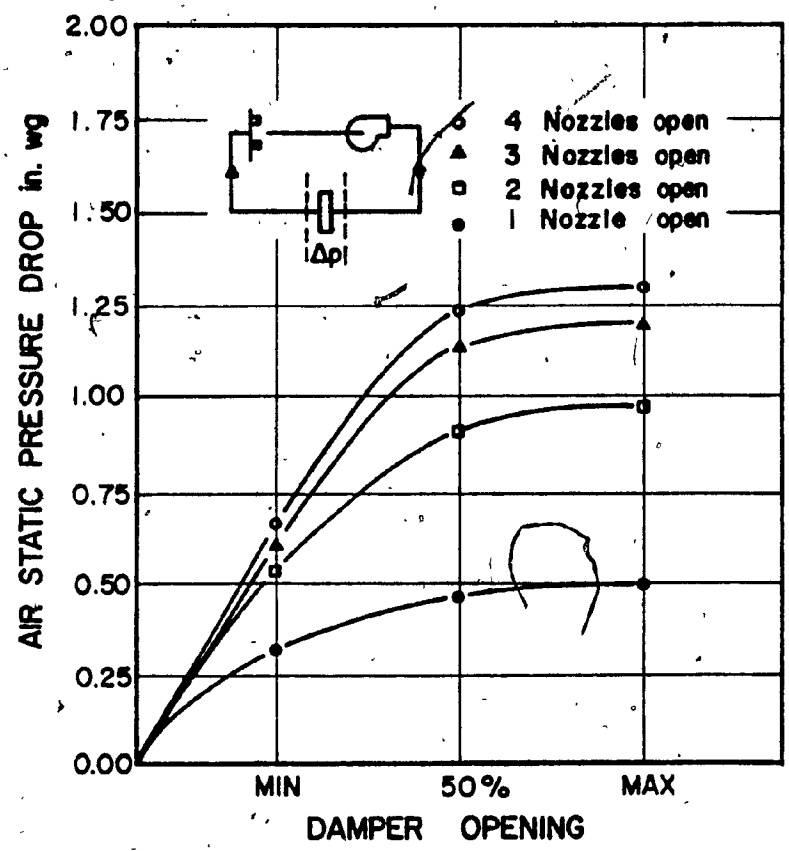

Figure 16 Air static pressure drops across the cooling coil for various damper positions.

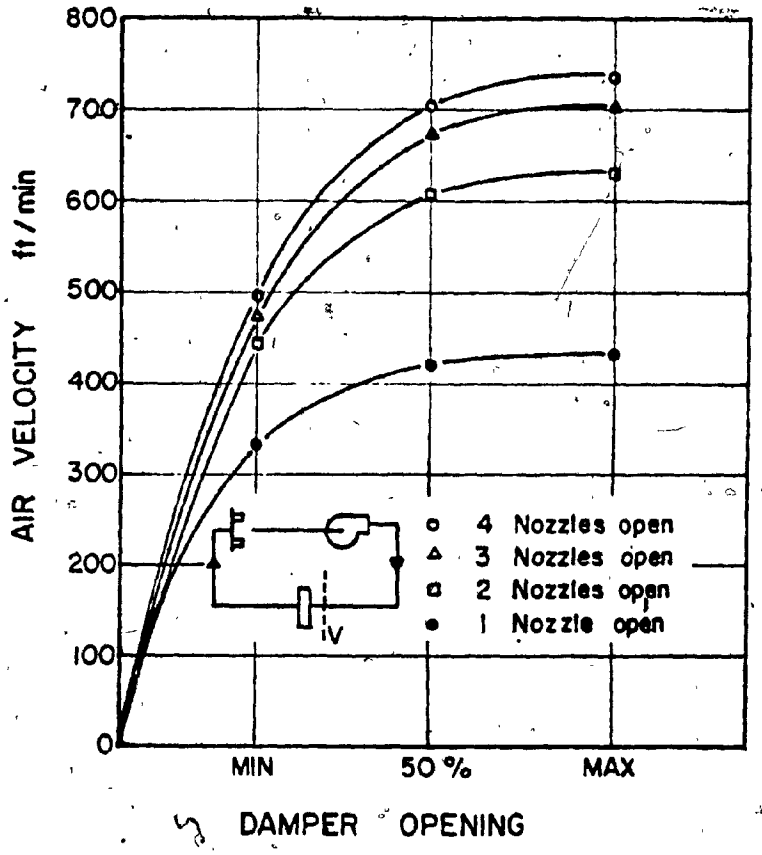

Figure 17 Cooling coil air face velocities for various damper positions.

CHAPTER 5

INSTRUMENTATION AND MEASUREMENTS

INSTRUMENTATION AND MEASUREMENT

In this section, the instrumentation requirements as stipulated in the standard (1) and the actual instrumentation and measurements systems used in the experiments are represented. A summary of the instrumentation used in the test is shown in Table 2 .

The instrumentation was selected based on performance characteristics and cost. Particular consideration was given to the adaptability of instruments to the automated data acquisition system.

5.1 Temperature Measuring Instruments [according to standard (1)]

Temperature of fluids within conduits shall be measured by inserting the temperature measuring instrument directly into the fluid stream or into a liquid-filled well inserted in the conduit. Glass thermometers should not be inserted directly into the fluid when the pressure within the conduit is great enough to affect the thermometer readings.

Table 3 shows the minimum requirements for accuracy and precision for temperature measuring instruments according to the standard (1).

ITEM	NO. OF MEASURE-MENT POINTS	TYPE OF MEASURING INSTRUMENT	RANGE OF OPERATION	ACCURACY REQUIRED	auto. DATA COLLECTION	non auto	COMMENTS
TEMPERATURE							
Air Dry Bulb Temp.	50	Shielded Copper Constant Thermocouple	-450 to+700°F	±0.1°F	✓		
Air Dry Bulb Temp. at Nozzles	4	Shielded Copper Constant Thermocouple, 24" PROBE	-450 to+700°F	±0.1°F	✓		high velocity
Refrigerant Temp.	2	RTD Platinum Resistance Thermometer	0 to+100°C	±0.5°F	✓		
Condenser Water Temp.	2	Remote Bulb Immersion Thermometer	+40 to+220°F	±0.5°F		✓	
Hot Water Temp.	2	Remote Bulb Immersion Thermometer	+40 to+220°F	±0.5°F		✓	
HUMIDITY							
Air Relative Humidity	2	Hygromechanical Actuated Strain Gauge Beam Sensor	-40 to+250°F	--	✓		"HY-CAL" special purpose sensor
PRESSURE							
Air Static Pressure	16	Strain Gauge Pressure Sensor	0-20" W.G.	1% of value	✓		
Refrigerant Pressure	2	Strain Gauge Pressure Sensor	0-300 PSI	±5% ABS.	✓		
TEMPERATURE & PRESSURE							
Refrigerant Temperature and Pressure	5	Standard Refrigeration Gauge	30VAC-300PSI -40 to+120°F	--		✓	control function only
FLOW							
Refrigerant Flow	1	Annular Averaging Velocity Head Sensor	0-30 GPM	±2% of value	✓		"ANNUBAR"
Condenser Water Flow	1	Annular Averaging Velocity Head Sensor	0-30 GPM	±1% of value	✓		"ANNUBAR"
Hot Water Flow	1	Annular Averaging Velocity Head Sensor	0-30 GPM	±1% of value	✓		"ANNUBAR"

TABLE 2 - Summary of Instrumentation Specifications

Measurement	Heating Coil Test	Cooling Coil Test	Remark
Wet and dry bulb temp	± 0.50°F	± 0.10°F	Air velocity 700 to 2000 FPM, preferably 1000 FPM
Water	± 0.50°F	± 0.10°F	or 2% of water temp drop if smaller
Other	± 0.50°F	±0.50°F	

TABLE 3

Air dry bulb temperature is measured by radiation shielded copper constantin thermocouples (24 gauge). The location of the thermocouple grids in the test chamber are shown in Fig. 18 .

Refrigerant temperature at various locations, as shown in Fig.19 , are measured by platinum resistance temperature sensors equipped with a linearized bridge amplifier and a scanner. Condensor water and heating coil water temperature are measured by remote bulb immersion thermometers (Power Regulator) fitted with silicon-gell filled wells.

5.2 Pressure Measuring Instruments:

Fluid Pressure measurements can be made with one or more of the following instruments:

a. Mercury column

b. Bourdan tube gauge

c. Manometer or draft gauge

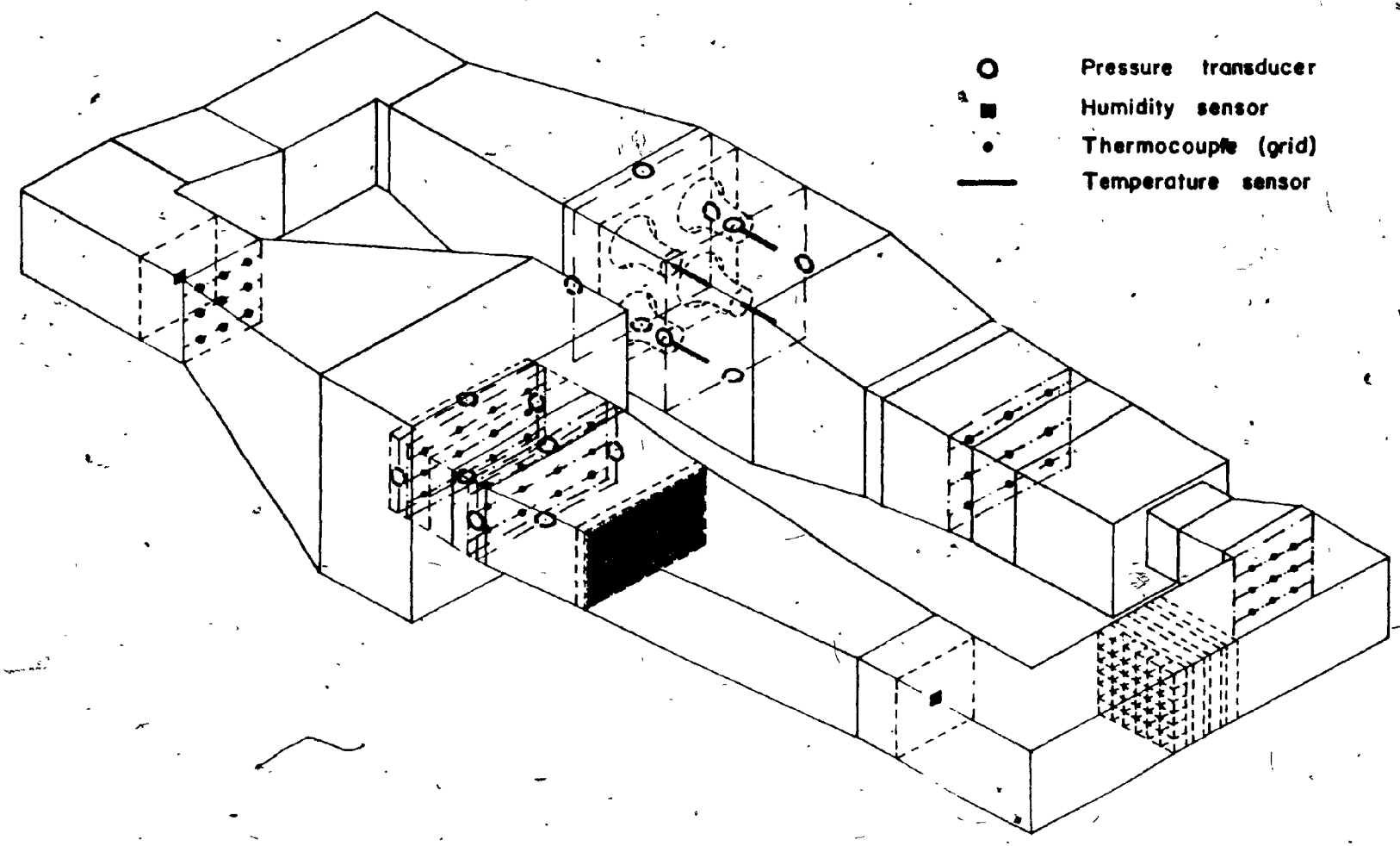

Figure 18 Heat exchanger performance test apparatus. Automatic air side instrumentation layout (cooling coil performance test).

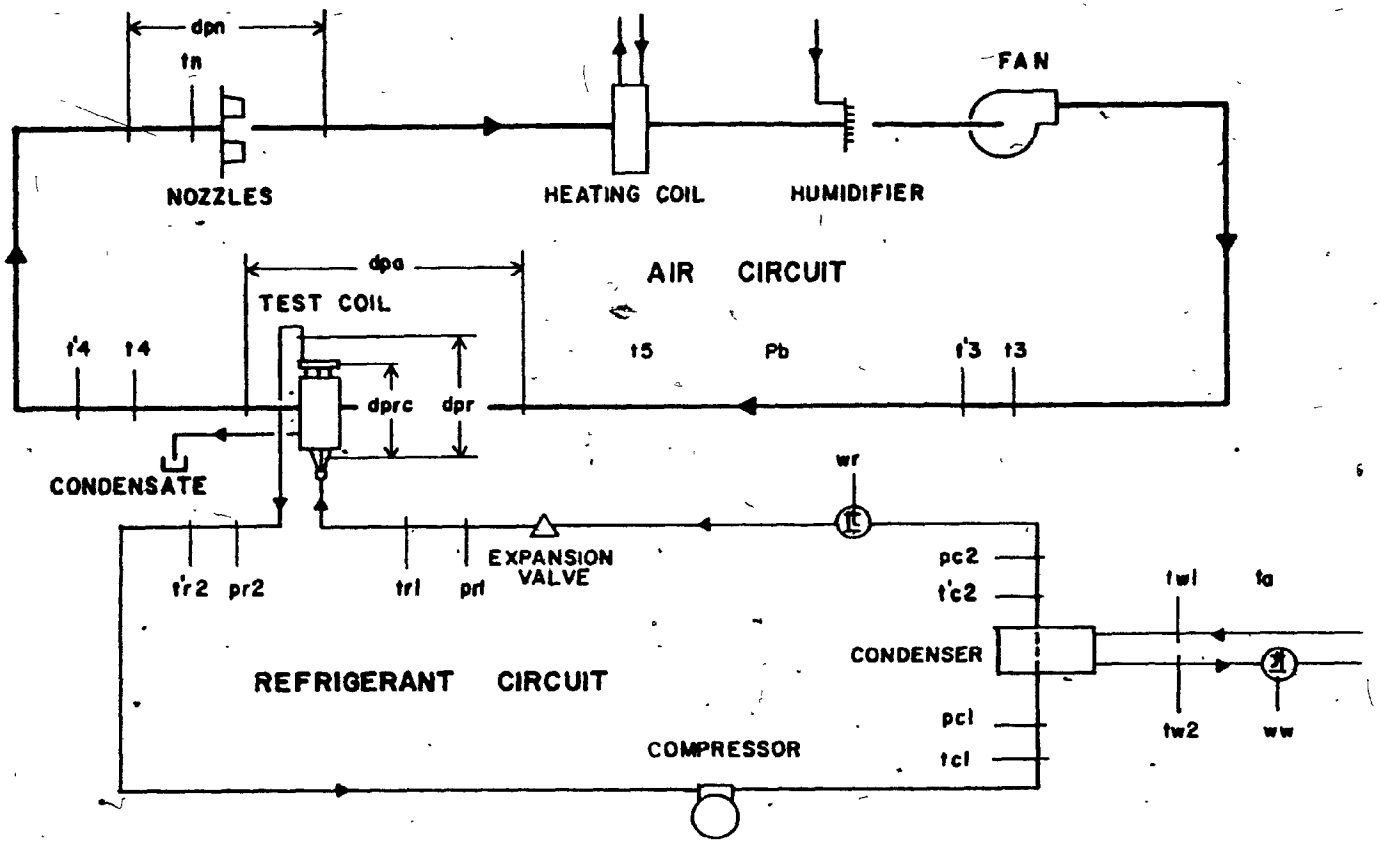

FIG. 19 Cooling Coil Performance Test Measurement Schematic Diagram

d. Pressure transducer

According to standards (1), the accuracy of the mercury columns or Bourdan tube guages shall permit pressure measurement within ± 0.5 percent absolute for refrigerant suction and within ± 2.0 percent absolute for all other pressures. Air static pressure and refrigerant pressure are measured by automatic strain-guage pressure transducers.

5.3 Air Flow Measuring Instrument

In this experiment air volume flow rate is measured by nozzles constructed in accordance with ASHRAE standard 33-78. Fig. 20 The velocity is obtained by measuring the static pressure drop across the nozzles using strain gauge type automatic air pressure transducers

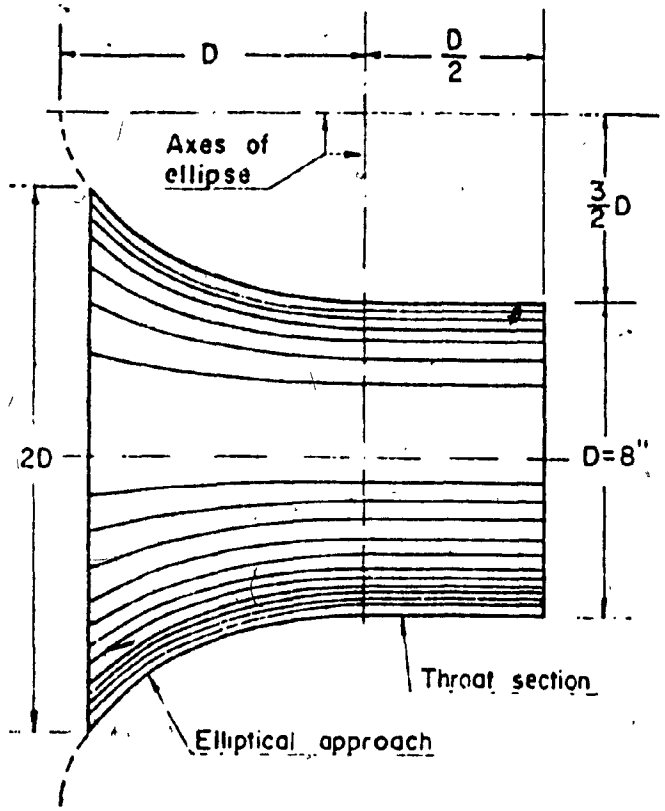

Figure 20 Airflow measuring nozzle. ASHRAE standard 33-78 section 5.1.6

5.4 Liquid Refrigerant, Condensor Water and Hot Water Measurement

The volitile refrigerant flow measuring shall be made [according to standard (1)] with one or more of the following instruments within the accuracy of ± 2.0 percent of the quantity measured:

a. Liquid flow meter method

b. Condensor water method

c. Calibrated compressor method

The details of these methods are described in the ASHRAE standard 33-78 (1). In this experiment refrigerant flow rate is measured, using both method "a" and "b" and the average value is used in the heat transfer calculations.

Water flow measurements shall be made [according to the standard (1)] with one or more of following instruments within an accuracy of ± 1% of the net quantity measured:

a. Liquid quantity meter

b. Liquid flow meter

(Liquid flow meter was used in this experiment)

Liquid refrigerant, condensor water and heating coil hot water flow rates are measured by "annubar" primary flow sensors. "Annubar" is an annular averaging velocity heat sensor for measurement of liquid flow (Fig. 21). Four annular parts of equal area on the upstream side and one part on the down stream side transmit differential velocity head signals through standard tubing to the two sides of a low displacement

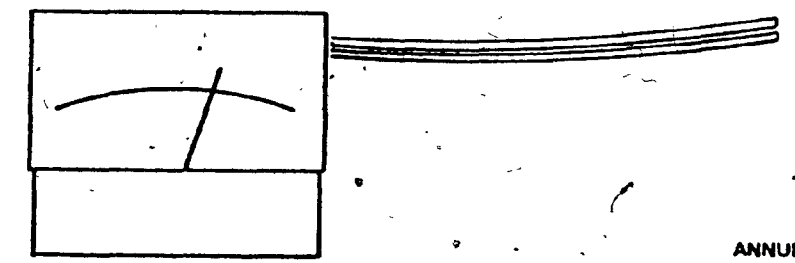

EAGLE EYE Flow Meter

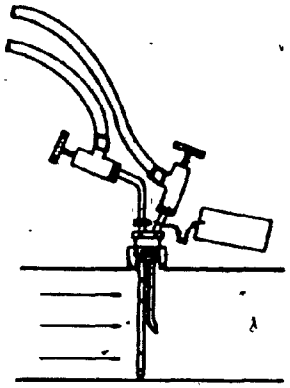

ANNUBAR
Flow Sensor

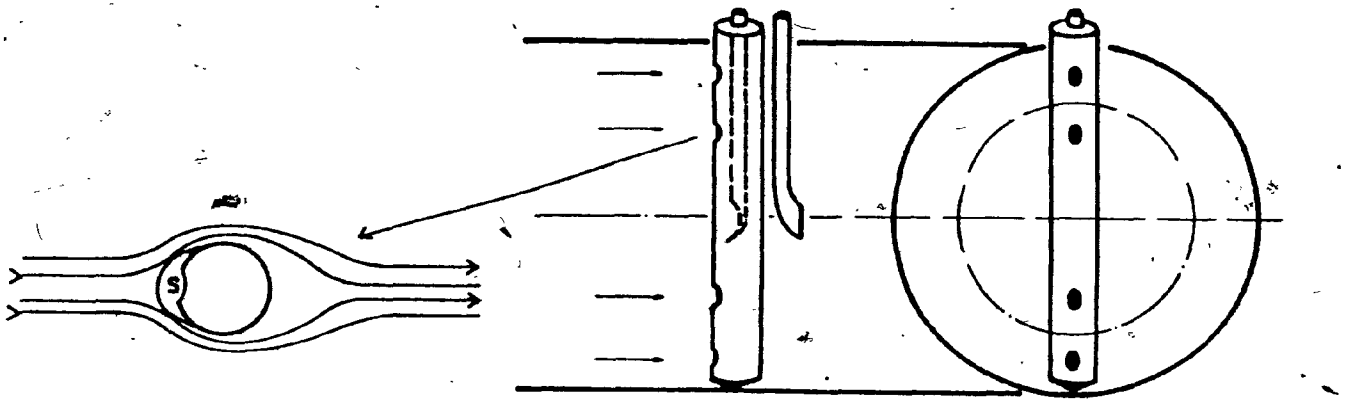

FIG. 21 Primary Flow Sensor and Meter

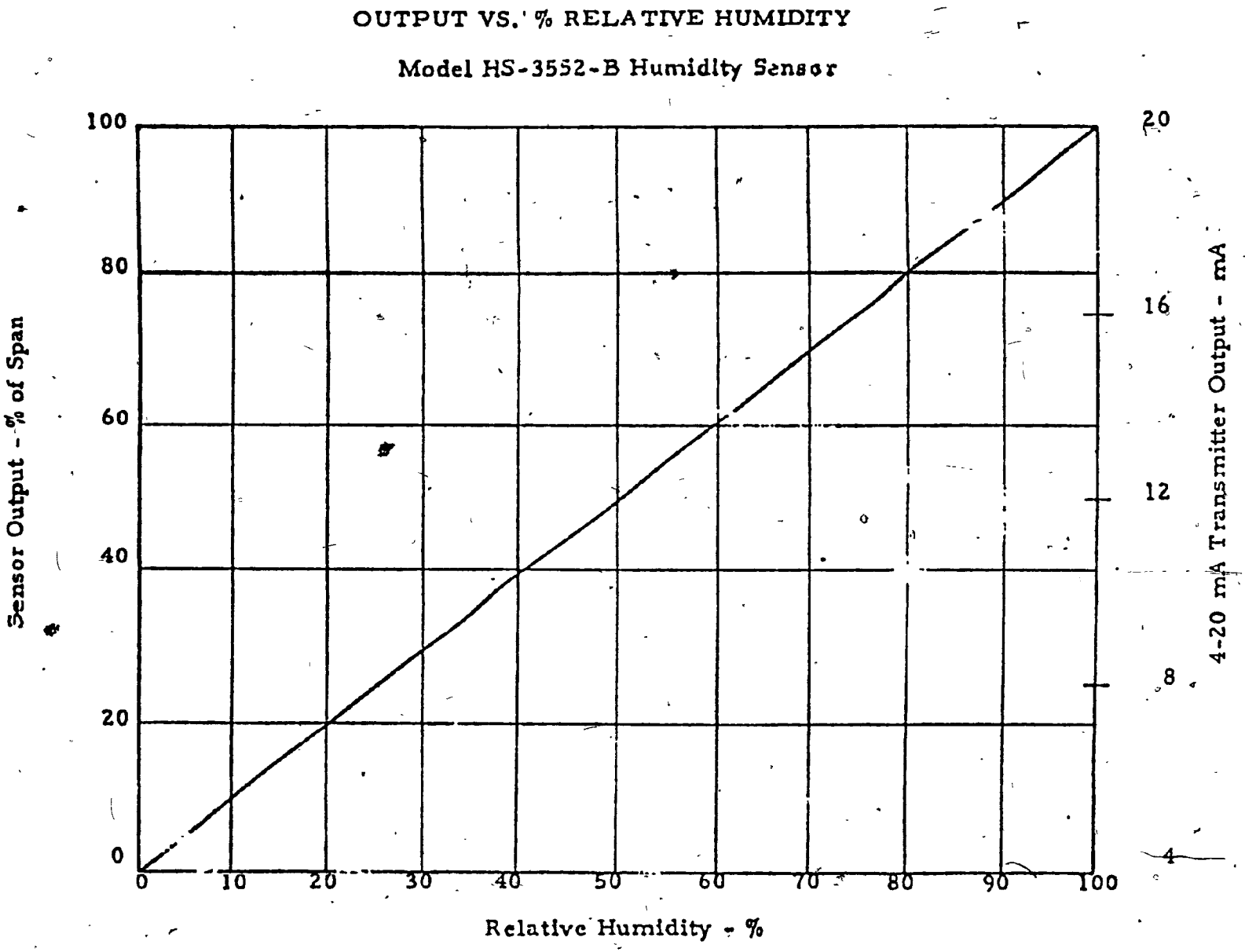

Figure 22. Calibration curve for humidity sensor

diaphragm. This diaphragm produces an axial motion which is transmitted through an adjustable range spring and a "flex-link" coupling. A permanent magnet connected to the range spring rotates proportional to the spring motion and a follower magnet located outside the pressure cavity follows the motion. A pointer connected to the follower magnet indicates flow. The relative motion between the two magnets is controlled by a patented technique to provide either linearized differential pressure or "normally linear" flow rate.

5.5 Air Relative Humidity

Air relative humidity is measured by a humidity sensor. This humidity sensor (model HS-3552-B by Hy-Cal Engineering) combines two components; a crystalline strip and a strain gauge beam. The driving element is a cellulose crystalline strip that reacts to humidity in much the same manner as a bimetal strip reacts to temperature. The action of the crystalline strip is used to hand the second component, a steel strip. The ends of the crystalline strip are attached to the steel strip with the outside of the curve toward the stainless strip. The two strain gauges attached to the beam from a half of bridge circuit for measuring bending strain which is proportional to the humidity change. The calibration curve of the humidity sensor is shown in Fig. 22 .

5.6 Data Acquisition System

In order to properly record a large number of measurements during the 45 minute test period, a data acquisition system was supplied for the

testing facility. Our requirements were for a portable 80 channel data logger with an instantaneous tape output and a facility to record data on a magnetic tape. This system includes:

a) A special zero reference section for copper constantin thermocouples with a linearizing circuit (50 channels).

b) Reference points for accepting signals from the linearizing transmitters from the resistance thermometers (2 channels).

c) Reference points for water gauge air static pressure transducers (16 channels).

d) Reference points for refrigerant pressure transducers (2 channels).

e) Reference points for "High-Cal" relative humidity transducers.

f) Reference points for high velocity air temperature measurement thermocouples.

g) Continuous scanning capability to scan all points at five, ten, fifteen or thirty minute intervals.

h) Built-in printer to keep a record of the data collected.

i) Provision for a hook-up to PDP-8 computer with disc or magnetic tape recorder (these hook-ups will be made for future tests).

j) Front panel control to isolate one or more sensors with an electronic display and printout for continuous measurement during set-up.

It is advisable to enclose the data acquisition system in a climate controlled chamber. The performance of the "reference junction" is affected considerably by extreme temperature and humidity conditions which would be

encountered in laboratories with self contained heating and cooling systems for the test chamber. A number of problems including complete system trip-off occured during these tests when the room humidity levels reaches 80% mark.

All thermocouples are connected to the reference junction assembly of the automatic data acquisition system. This reference junction assembly is designed to provide a uniform temperature throughout the thermocouple termination points. This thermal assembly is allowed to "float" at the ambient temperature. An integral temperature sensing diode measures the temperature accurately at any given time and produces a correction voltage with respect to a reference temperature. This correction voltage is then applied to low input terminals, thereby maintaining a constant reference junction temperature at all times.

This technique also permits intermixing of different types of thermocouples in one experiment. The thermocouple linearization is performed digitally with "look-up" tables (N.B.S. Mongraph #125) stored in hard ware of the unit.

CHAPTER 6

TEST PROCEDURE AND DISCUSSION OF RESULTS

6.1 Description of the Test Procedure

The test coil and a 'matching' heating coil are installed at the designated locations in the test chamber (Fig. 10). Necessary piping connections are made and the measuring instruments are installed in the appropriate positions (Fig. 19). With the coils, and instrumentation in their respective positions the "air side performance" data for the test chamber is experimentally determined as shown in Chapter 3.

The performance tests for the coil are conducted for one set inlet air conditions (80°F (26.7°C) D.B., 67°F (19.4°C) W.B.) to facilitate comparison of the experimental data with the performance data published by the manufacturer. The intake air conditions are maintained automatically by a thermostat controlling the hot water flow rate into the heating coil and a humidistat controlling the steam flow rate into the humidifier (Fig. 12). The refrigerant flow rate for various loads is controlled automatically by a thermostatic expansion valve that maintains a constant 12°F (6.67°C) superheat at the coil exit. Refrigeration capacity control is achieved by the hotgass-by-pass method (Fig. 11).

By manipulating the variable volume fan, the coil face velocities are varied in 6 steps from 179.6 to 436.9 FPM (0.912 t_p 2.33 m/sec). The average face velocity at the coil for each test is determined by pitot-tube traverse method for rectangular ducts (38). For each of the designated face velocities, after a steady state is reached, all of the automatic measurements are recorded by a data acquisition system, at 5

minute intervals, for the test period of 45 minutes. A sample of velocity profile is shown in the appendix 3.

6.2 Discussion of Test Results

A summary of the input and output data are shown in Tables 23 and 24 in the appendix. All the performance data graphs are shown in Figures 22 to 25.

The air mass flow rates corresponding to the 6 face velocities varied from 101.01 to 245.76 lb/min. (0.764 to 1.86 kg/sec dry air). Higher face velocities could not be tested due to limitations in the refrigeration system capacity (10 tons, (35.2 K.W.)). Subsequently, this refrigerant system is replaced by a 25 tons (88 K.W.) system with cylinder unloading type capacity control.

The refrigerant mass flow rates for these face velocities at constant intake air conditions varied from 1100 to 1915 $lb/_{hr}$ (138.6 to 241.3 g/sec.). The refrigerant suction temperature varied from 29.81°F to 34.83°F (-1°C to 1.3°C). The refrigerant superheat in the suction header varied from 12°F - 13°F (6.7°C to 7.3°C) which is very close to the limits recommended by the standard (1).

The average total heat capacity of the coil varied from 6.64 to 11.93 tons (23.37 to 41.99 K.W.). For the same range, the capacity reported by the manufacturer varied from 6.9 to 11.93 tons (24.29 to 41.18 K.W.). The average difference over the full range between the

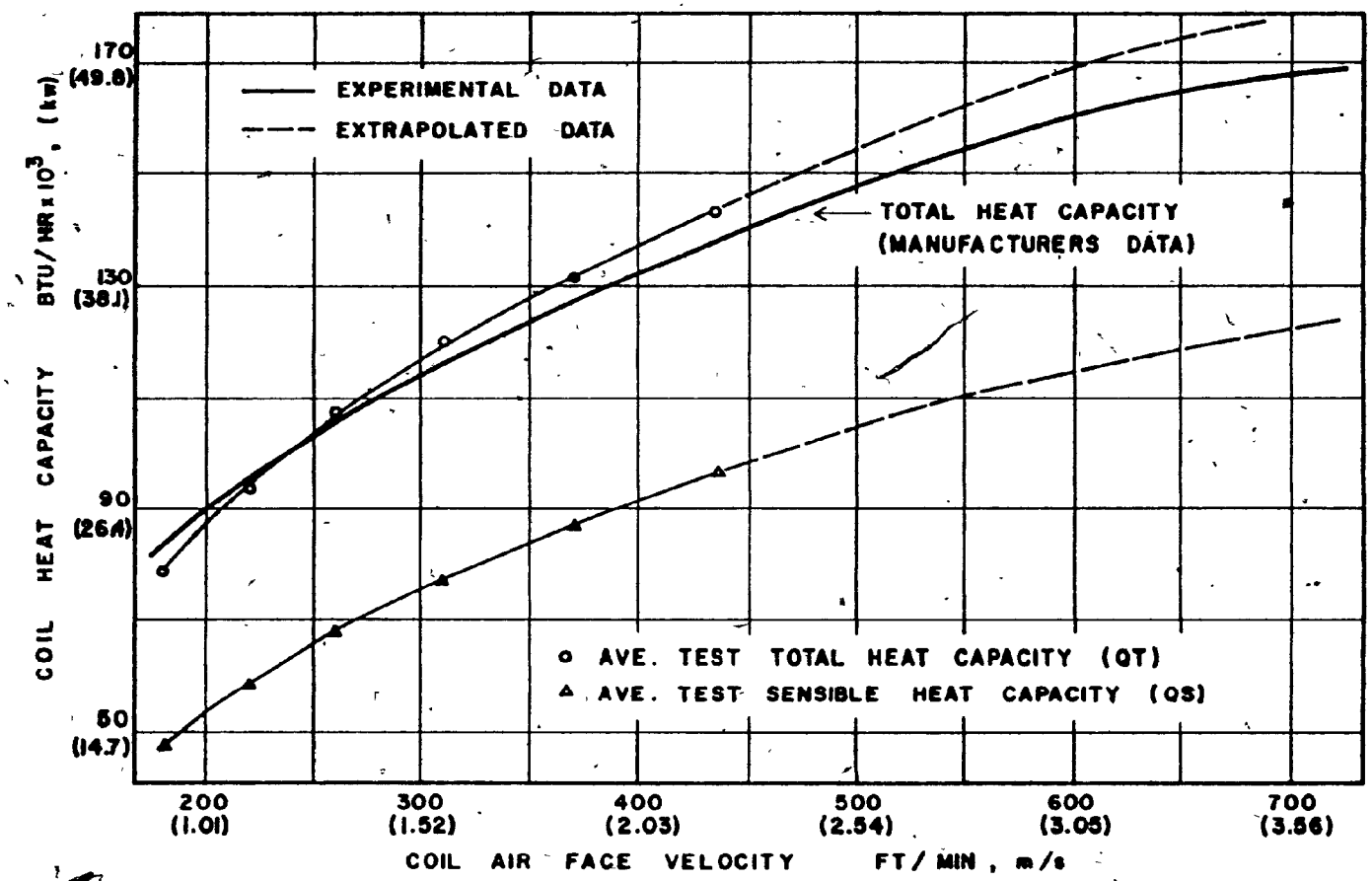

FIG. 22 Average Test Total, Sensible and Manufacturers Data on Heat Capacities

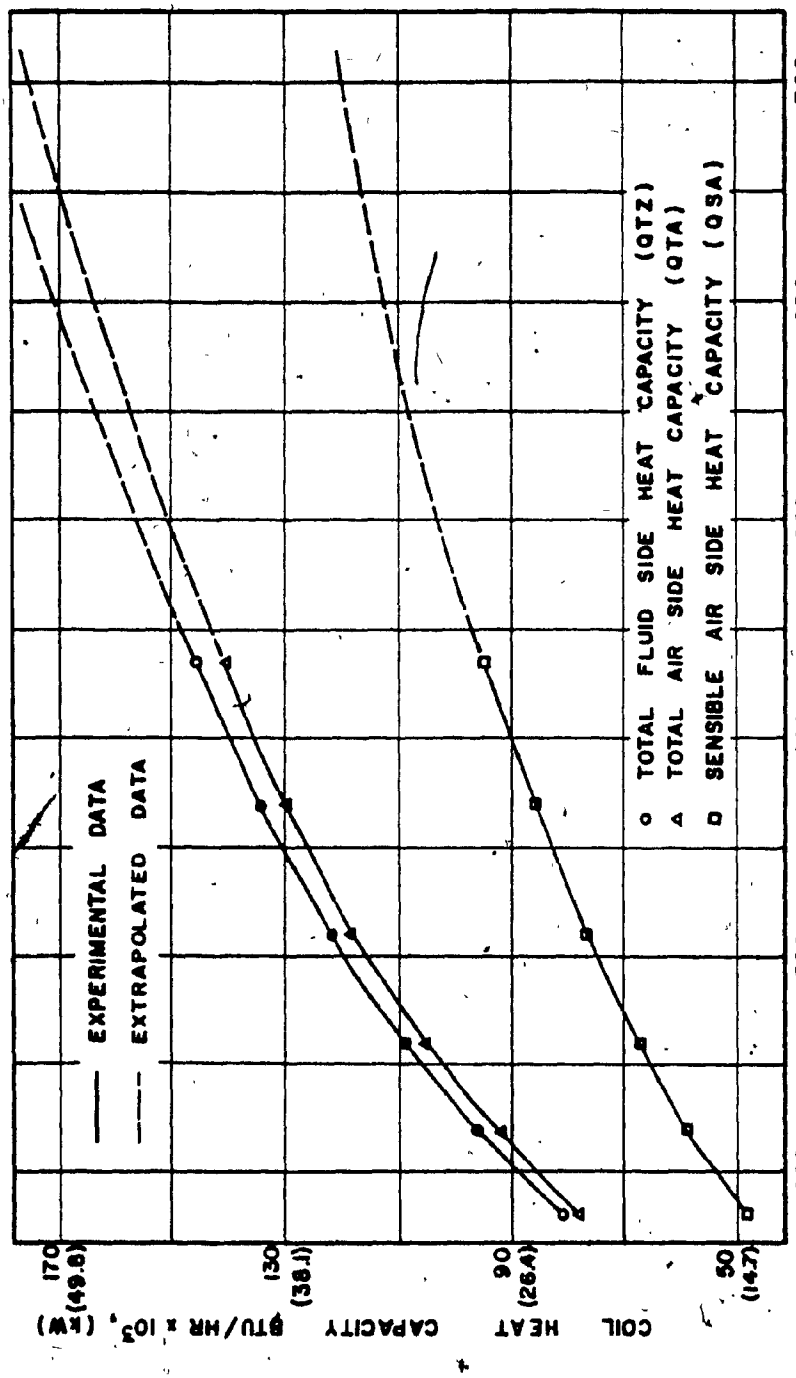

FIG. 23 Total and Sensible Heat Capacities

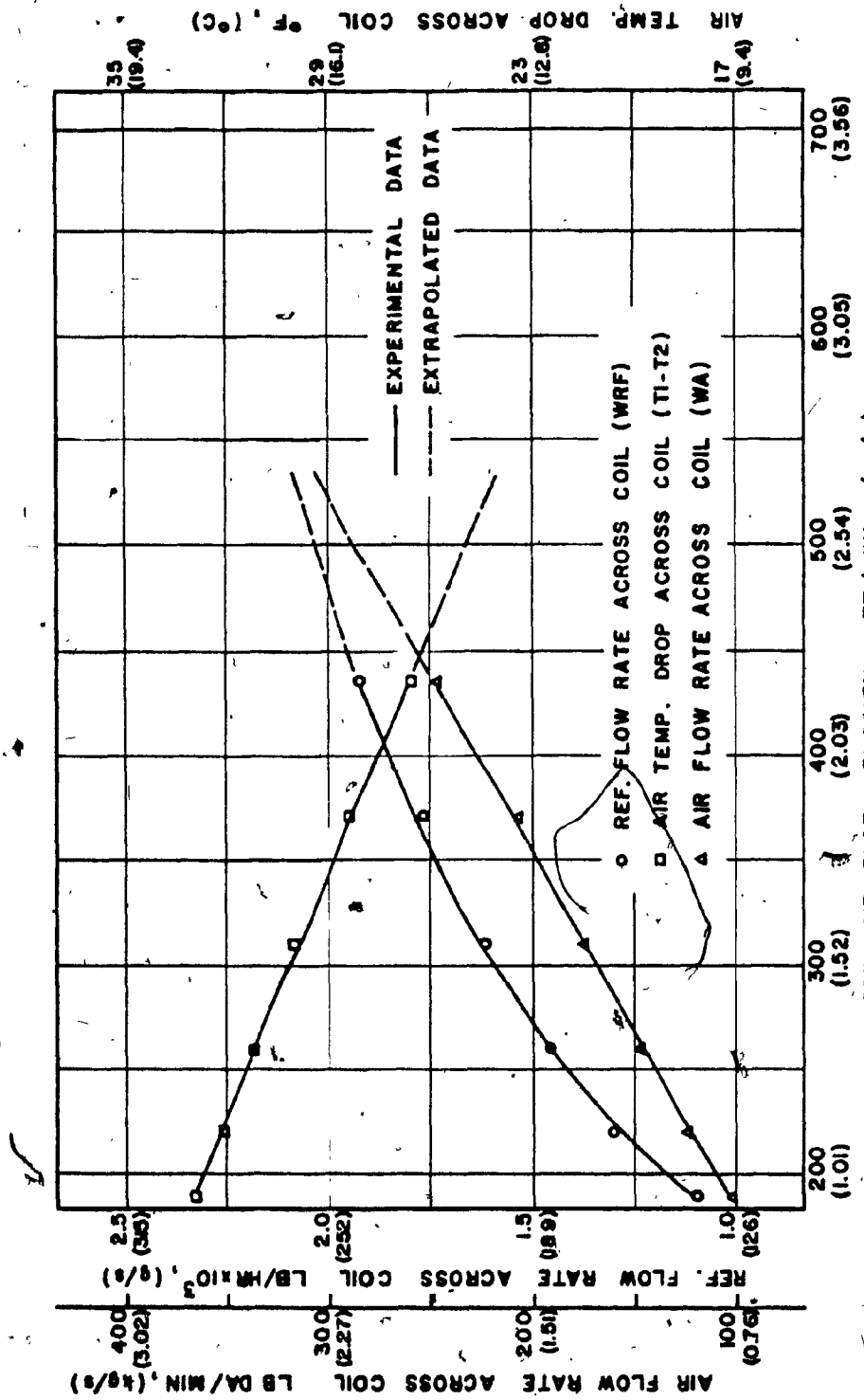

FIG. 24 Air and Refrigerant Flow Rates and Air Temperature Drop Across Coil

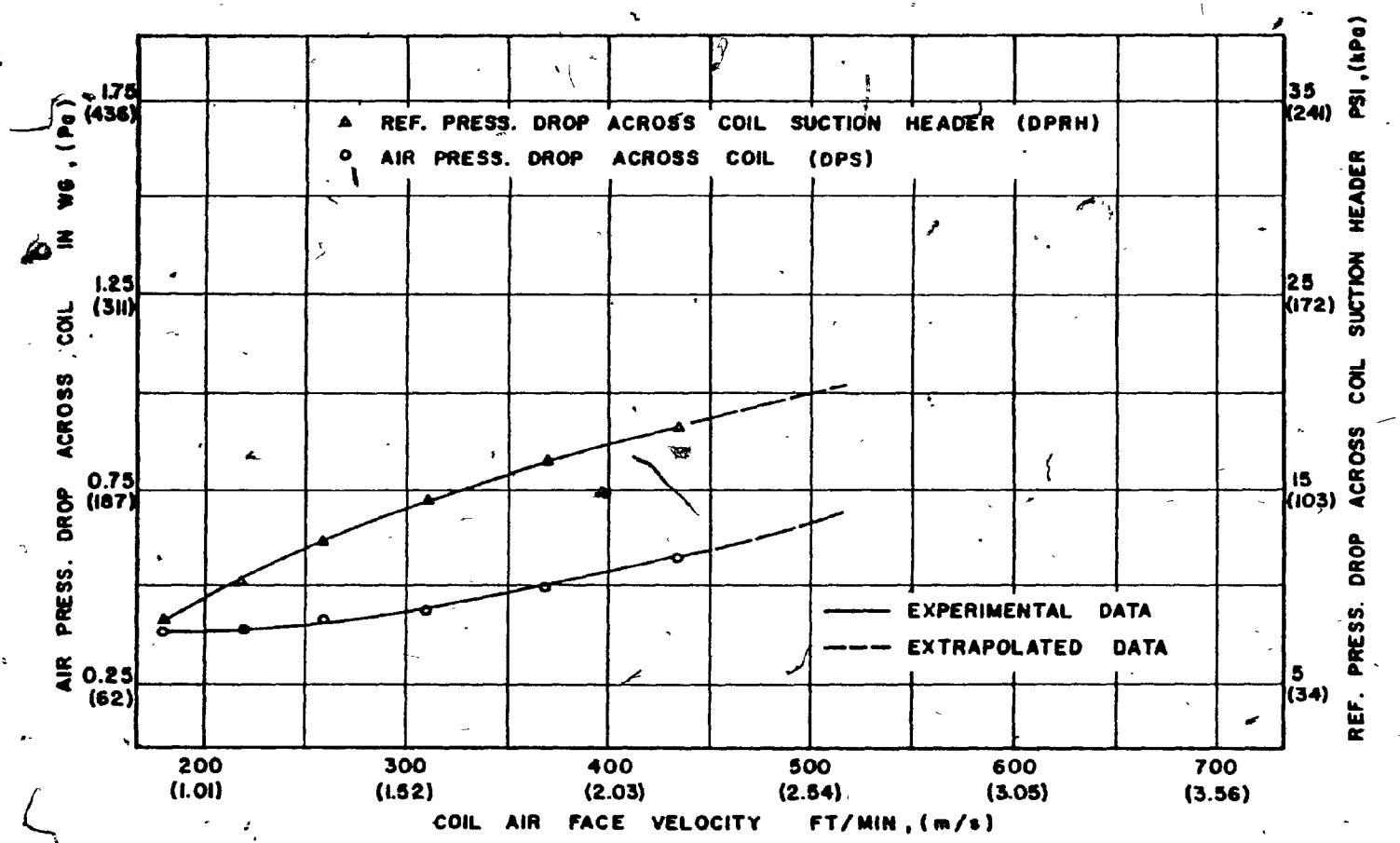

FIG. 25 Air and Refrigerant Pressure Drops

experimental data and manufacturer's data is 2.84 percent, indicating a fairly good agreement for this coil and for this range of operation. The experimental heat balance (HBT) between the air side and refrigerant side heat capacities varied from a minimum of -1.28% for test 'D' to a maximum of -3.9% for test 'B' as shown in Table 23. This value is well within the 5% variation limit recommended by the standard (1).

Air and refrigerant pressure drop data across the test coil (Fig. 25) also matched closely with the data reported by the manufacturer.

CHAPTER 7

CONCLUSION

CONCLUSION

The test results indicated a close agreement between the performance data published by the manufacturer and the experimental data.

To examine the part load performance of the coil, the major heat transfer parameters (Q_{au}, ΔP_{rh}, ΔP_s and W_r) are expressed as a percentage of the full load value. The full load value represents the value of the given parameter at the full load condition represented by the corresponding air face velocity of 436.9 f.p.m. (2.22 m/s). The percentage values of these parameters are plotted against the corresponding percentage load as shown in Fig. 26. From Fig. 26 as the percentage load increase, the percentage value of the parameters W_r, Q_{au}, and ΔP_{rh} increases gradually as one would expect. However, air pressure drop across the coil, (ΔP_s), increased gradually up to about the 70 percent load value and then a sudden increase is observed beyond this point. (Fig. 26) The Reynolds number for air flow at the variation point (70%) is about 404. This sudden increase in pressure drop may be attributed to the beginning of turbulance at the given face velocity for the given configuration.

Normally, the air flow Reynolds number, for air cooling and dehumidifying applications (for comfort) is in the range of 200-1500. The heavy turbulance and possible moisture carry over could occur in the

higher range or Reynold's number (1200 and above).

To further investigate this abnormal pressure drop phenomena at relatively low Reynold's number for air flow (400), it is necessary to obtain additional experimental data.

The following is the proposed experimental programme for the investigation of the pressure drop variations:

1. Performance evaluation to be conducted for higher range of air face velocities (up to 800 F.P.M.) for this (4 Row, 12 FPI) Coil.

2. Using the same face area, tube diameter and fin spacing evaluate the performance of 3, 6 and 8 Row Coils.

3. With same face area, tube diameter and number of rows (4 rows) evaluate performance of 6, 8 and 10 fin per inch coils.

Upon satisfactory completion of these tests, one will be in a better position to understand the heat transfer and pressure drop variation on the coil as a function of the major coil construction parameters (fin and tube spacing). These tests are currently being carried out at CBS laboratories.

Fig. 26 Coil part load performance data
(expressed as percentage of full load)

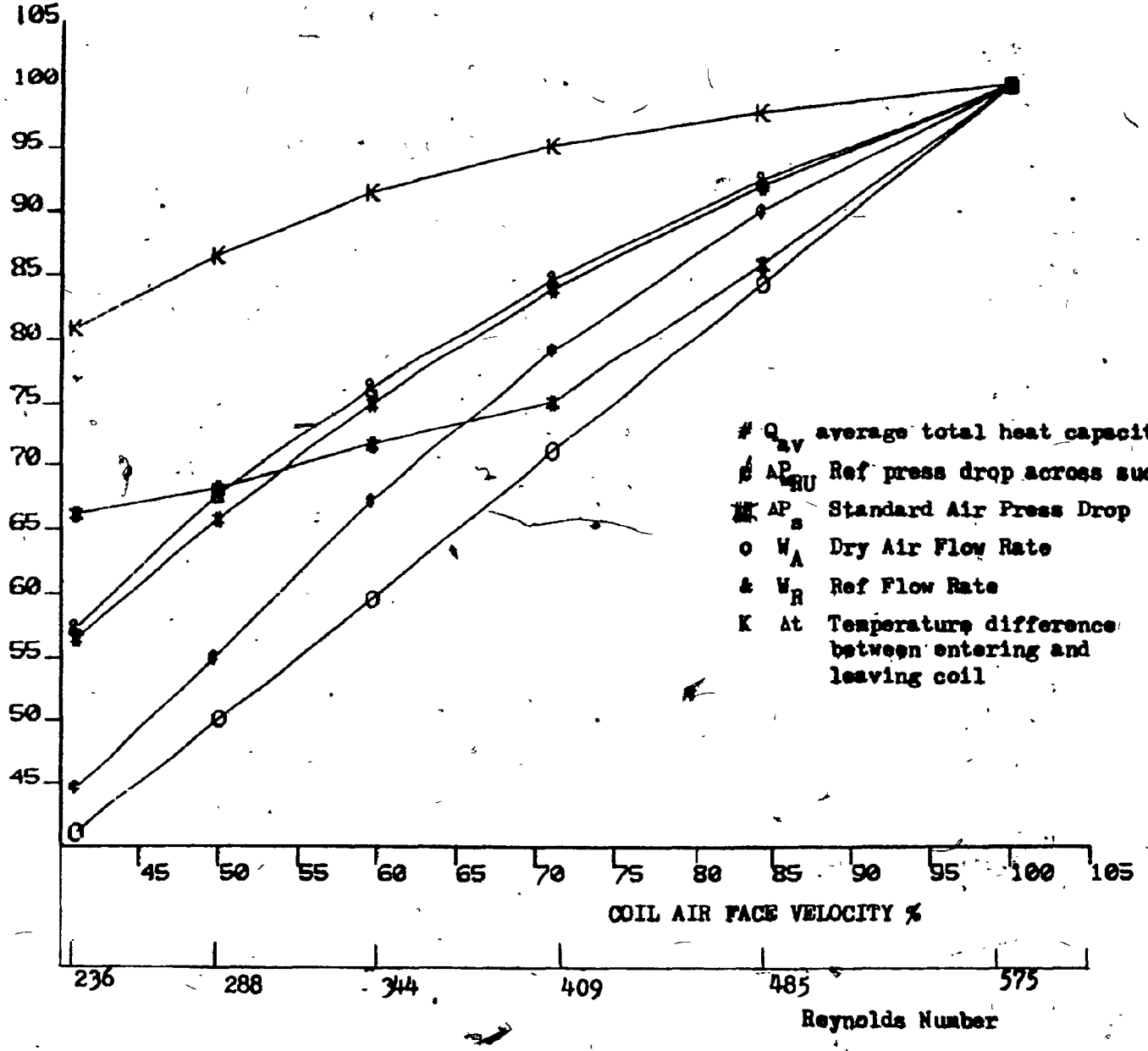

CHAPTER 8

UNCERTAINTY ANALYSIS

UNCERTAINTY ANALYSIS

8.1 Introduction

In this section, the uncertainty analysis in the anticipated test results are discussed. Statistical techniques provide methods for dealing economically with a representative sample of a large number of Data. For most of engineering cases, it is too costly and impractical to perform a true multisample experiment. However, repeated measurements with the same instrumentation and the same observer may provide a fair approximation of a multisample experiment. The uncertainties involved in the test results are obtained by the well known methods of statistics as described in ASHRAE standard (11).

8.2 Analysis of the Air Dry Bulb Temperature Measurement Entering the Coil

A sample series of thermo-couple reading for dry bulb temperature entering the coil, recorded by the data acquisition system are shown in Table 12. The calculation for the standard deviation, mean deviation or probable error, standard deviation of the mean and estimation of the uncertainty according to the normal probability curve are described.

TABLE 12

Reading Number	Dry Bulb Temp.
1	26.4 $^{o}_{C}$
2	26.3
3	26.4
4	26.4
5	26.3
6	26.3
7	26.2
8	25.8
9	26.3
10	26.3
11	26.3
12	25.9
13	27.1
14	27.5
15	27.7
16	27.6
17	26.2
18	27.8
19	27.6
20	27.5
21	27.3
22	27.4
23	27.7
24	27.4
n = 24	$\sum x_i = 644$

From Table 12 the mean value of the temperature :

$$\bar{X} = \frac{1}{n} \sum_{i=1}^{n} X_i = \frac{1}{24} (644) = 26.83$$

The following Table aids in computing mean deviation and standard deviation.

Reading	$X_i - \bar{X}$	$(X_i - \bar{X})^n$
1	-0.43	0.1849
2	-0.53	0.2809
3	-0.43	0.1849
4	-0.43	0.1849
5	-0.53	0.2809
6	-0.53	0.2809
7	-0.63	0.3969
8	-1.03	1.0609
9	-0.53	0.2809
10	-0.53	0.2809
11	-0.53	0.2809
12	-0.93	0.8649
13	0.27	0.0729
14	0.67	0.4489
15	0.87	0.7569
16	0.77	0.5929
17	-0.63	0.3969
18	0.97	0.9409
19	0.77	0.5929
20	0.67	0.4489
21	0.47	0.2209
22	0.57	0.3249
23	0.87	0.7569
24	0.57	0.3249
$n = 24$	$\sum \lvert X_i - \bar{X} \rvert = 15.16$	$\sum (X_i - \bar{X})^2 = 10.4416$

TABLE 13

The standard deviation is

$$\sigma = \frac{1}{n} \sum_{i=1}^{n} \left[(X_i - \bar{X})^2 \right]^{\frac{1}{2}} = \frac{1}{24} (10.4416)^{\frac{1}{2}} = 0.14^{OC}$$

The average of the reading is 26.83^{OC} and the standard deviation is 0.14^{OC}. The mean deviation or probable error is :

$$\bar{d}_i = \frac{1}{n} \sum_{i=1}^{n} \left| d_i \right| = \frac{1}{n} \sum_{i=1}^{n} \left| X_i - \bar{X} \right|$$

$$= \frac{1}{24} (15.16) = 0.64^{OC}$$

The standard deviation of the mean is :

$$\bar{\sigma} = \frac{\sigma}{\sqrt{n}} = \frac{0.14}{\sqrt{24}} = 0.029$$

The arithmetic mean value was 26.83^{OC} with the final result reported in terms of the uncertainty as :

$\bar{X}$	=	26.83 ± 0.029^{OC}	68.3%
$\bar{X}$	=	26.83 ± 0.058^{OC}	95 %
$\bar{X}$	=	26.83 ± 0.087	99.7%

Dry Bulb Temperature Leaving The Coil

A sample series of thermocouple readings for DB temperature leaving the coil are shown in Table 14 . On the basis of the t - distribution, an estimate of the true value of variable 'X' can be expressed as:

$$\bar{X} = \bar{X}' \pm \frac{t \sigma'}{\sqrt{n}}$$

According to ASHRAE standard 41.5.75, (page 7) in the formula of standard deviation, if n < 20, (n - 1) is substituted instead of n and the symbol σ' is used to indicate an estimate of σ . Therefore, σ' is:

$$G' = \left[\frac{1}{n-1} \sum_{i=1}^{n} (X_i - \bar{X}')^2 \right]^{\frac{1}{2}}$$

The value of t is tabulated in Table 15 as a function of the degrees of freedom and the desired degree of confidence. Degrees of freedom can be defined in general as the number of observations minus the number of different quantities estimated.

Reading	Dry Bulb Temperature	$X_i - \bar{X}$	$(X_i - \bar{X})^2$
1	12.2	[illegible]	0.0484
2	11.1°C	-0.88	0.7744
3	11.2	-0.78	0.6084
4	11.9	-0.08	0.0064
5	12.1	0.12	0.0144
6	11.8	-0.18	0.0324
7	11.7	-0.28	0.0784
8	12.2	0.22	0.0484
9	12.3	0.32	0.1024
10	11.2	-0.78	0.6084
11	11.6	-0.38	0.1444
12	12.3	0.32	0.1024
13	12.2	0.22	0.0484
14	12.4	0.42	0.1764
15	12.0	0.02	0.004
16	12.4	0.42	0.1764
17	12.8	0.82	0.6724
18	12.3	0.32	0.1024
n = 18	$\sum X_i = 215.7$	$\sum \lvert X_i - \bar{X} \rvert = 6.78$	$\sum (X_i - \bar{X})^2 = 3.7452$

TABLE 14

Table I.5

Degrees of Freedom	Student's t: P, Probability of Obtaining a Given Value of t (or a Larger One)							
	0.50	0.20	0.10	0.05	0.02	0.01	0.001	0.0005
1	1.000	3.078	6.314	12.706	31.821	63.657	318.310	636.620
2	0.817	1.886	2.920	4.303	6.965	9.925	22.326	31.598
3	0.765	1.638	2.353	3.183	4.541	5.841	10.213	12.924
4	0.741	1.533	2.132	2.776	3.747	4.604	7.173	8.610
5	0.727	1.476	2.015	2.571	3.365	4.032	5.893	6.869
6	0.718	1.440	1.943	2.447	3.143	3.707	5.208	5.959
7	0.711	1.415	1.895	2.365	2.998	3.500	4.785	5.408
8	0.706	1.397	1.860	2.306	2.896	3.355	4.501	5.041
9	0.703	1.383	1.833	2.262	2.821	3.250	4.297	4.781
10	0.700	1.372	1.813	2.228	2.764	3.169	4.144	4.587
11	0.697	1.363	1.796	2.201	2.718	3.106	4.025	4.437
12	0.695	1.356	1.782	2.179	2.681	3.055	3.930	4.318
13	0.694	1.350	1.771	2.160	2.650	3.012	3.852	4.221
14	0.692	1.345	1.761	2.145	2.624	2.977	3.787	4.140
15	0.961	1.341	1.753	2.132	2.602	2.947	3.733	4.073
16	0.690	1.337	1.746	2.120	2.583	2.921	3.686	4.015
17	0.689	1.333	1.740	2.110	2.567	2.898	3.646	3.965
18	0.688	1.330	1.734	2.101	2.552	2.878	3.610	3.922
19	0.688	1.328	1.729	2.093	2.539	2.861	3.579	3.883
20	0.687	1.325	1.725	2.086	2.528	2.845	3.552	3.850
21	0.686	1.323	1.721	2.080	2.518	2.831	3.527	3.819
22	0.686	1.321	1.717	2.074	2.508	2.819	3.505	3.792
23	0.685	1.319	1.714	2.069	2.500	2.807	3.485	3.767
24	0.685	1.318	1.711	2.064	2.492	2.797	3.467	3.745
25	0.684	1.316	1.708	2.060	2.485	2.787	3.450	3.725
26	0.684	1.315	1.706	2.056	2.479	2.779	3.435	3.707
27	0.684	1.314	1.703	2.052	2.473	2.771	3.421	3.690
28	0.683	1.313	1.701	2.048	2.467	2.763	3.408	3.674
29	0.683	1.311	1.699	2.045	2.462	2.756	3.396	3.659
30	0.683	1.310	1.697	2.042	2.457	2.750	3.385	3.646
40	0.681	1.303	1.684	2.021	2.423	2.705	3.307	3.551
60	0.679	1.296	1.671	2.000	2.390	2.660	3.232	3.460
120	0.677	1.289	1.658	1.980	2.358	2.617	3.160	3.373
∞	0.674	1.282	1.645	1.960	2.326	2.576	3.090	3.291

The mean value is :

$$\bar{X} = \frac{1}{n} \sum_{i=1}^{n} X_i = \frac{1}{18} (215.7) = 11.98$$

$$\sigma' = \left[\frac{1}{18-1} (3.7452) \right]^{\frac{1}{2}} = 0.47^{OC}$$

On the basis of the t-distribution, an estimate of the time value of n is :

$$X = \bar{X} \pm \frac{t\, \sigma'}{\sqrt{n}}$$

For the 17 degrees of freedom of this case and the recommended confidence level of 95 percent, from Table 15 : t = 2.110

And the estimate of the true value of X becomes :

$$X = 11.98 \pm \frac{2.110(0.47)}{\sqrt{18}} = 11.98 \pm 0.23^{OC}$$

with the final result reported as :

X = 11.98 ± 0.23 95 percent.

8.3 Analysis of the Air Humidity Measurements Before and After Cooling Coil

Table 16 shows a sample series readings for percentage of humidity taken by this humidity sensor and recorded by data acquisition system. According to Chauvenets method (11) all points whose ratio of deviation to trial standard deviation are higher than that given in Table 17 are rejected, and a new mean and standard deviation is then computed with the rejected points eliminated.

a) Humidity Before C/C

Reading	Humidity	$X_i - \bar{X}$	$(X_i - \bar{X})^2$
1	44.8%	0.3	0.09
2	44.4%	-0.1	0.01
3	44.2%	-0.3	0.09
4	44.5%	0	0
5	44.6%	0.1	0.01
6	44.6%	0.1	0.01
7	44.3%	-0.2	0.04
8	44.4%	-0.1	0.01
9	44.6%	0.1	0.01
10	44.6%	0.1	0.01
11	44.2%	-0.3	0.09
12	44.6%	0.1	0.01
13	44.7%	0.2	0.04
n=13	$\sum X_i = 578.5$	$\sum \lvert X_i - \bar{X} \rvert = 2.0$	$\sum (X_i - \bar{X})^2 = 0.42$

TABLE 16

The mean value is :

$$\bar{X} = \frac{1}{n} \sum_{i=1}^{n} X_i = \frac{1}{13} (578.5) = 44.5\%$$

$$\sigma = \hat{\sigma} = \frac{1}{n-1} \sum_{i=1}^{n} \left[(X_i - \bar{X})^2 \right]^{\frac{1}{2}} = \frac{1}{12} (0.42)^{\frac{1}{2}} \approx 0.05\%$$

*TABLE 17

Chauvenet's Criterion for Rejecting a Reading

Number of Readings. n	Ratio of Maximum Acceptable Deviation to Standard Deviation, dmax/a
2	1.15
3	1.38
4	1.54
5	1.65
6	1.73
7	1.80
10	1.96
15	2.13
25	2.33
50	2.57
100	2.81
300	3.14
500	3.29
1,000	3.48

* Extracted from (11)

Reading	d_i/σ	Reading	d_i/σ
1	0.06	8	0.02
2	0.02	9	0.02
3	0.06	10	0.02
4	0.00	11	0.06
5	0.02	12	0.02
6	0.02	13	0.04
7	0.04		

TABLE 18

In accordance with Table 18 for 13 readings, readings with values of $d_i/\sigma > 2.05$ are questionable. Thus, no reading in this set is questionable.

On the basis of the t-distribution, an estimate of the true value of n is :

$$X = \bar{X} \pm \frac{t\sigma}{\sqrt{n}}$$

For the 12 degrees of freedom of this case and the recommended confidence level of 90%, from Table 15 : $t = 1.782$, therefore

$$\bar{X} = 44.5\% \pm \frac{1.782 \times 0.05}{\sqrt{13}} = 44.5\% \pm 0.02$$

with the final result reported as :

$X = 44.5\% \pm 0.02$, 90 percent

b) Humidity After C/C

Reading	Humidity	$X_i - \bar{X}$	$(X_i - \bar{X})^2$
1	95.1%	0.22	0.0484
2	94.9%	0.02	0.0004
3	94.9%	0.02	0.0004
4	94.9%	0.02	0.0004
5	94.9%	0.02	0.0004
6	94.9%	0.02	0.0004
7	94.8%	-0.08	0.0064
8	94.7%	-0.18	0.0324
9	94.8%	-0.08	0.0064
10	95 %	0.12	0.0144
11	94.8%	-0.08	0.0064
12	94.8%	-0.08	0.0064
13	94.9%	0.02	0.0004
n=13	$\sum X_i = 1233.4$	$\sum \lvert X_i - \bar{X} \rvert = 0.96$	$\sum (X_i - \bar{X})^2 = 0.1232$

TABLE 19

The mean value is :

$$\bar{X} = \frac{1}{n} \sum_{i=1}^{n} X_i = \frac{1}{13} (1233.4) = 94.88\%$$

$$\sigma = \sigma = \frac{1}{n-1} \sum_{i=1}^{n} \left[(X_i - \bar{X})^2 \right]^{\frac{1}{2}} = \frac{1}{12} (0.1232)^{\frac{1}{2}} = 0.03\%$$

The same procedure as the previous example, non of readings is questionable.

By use of Table 15, for confidence level of 95% :

$$\bar{X} = 94.88 \pm \frac{1.782 \times 0.03}{\sqrt{13}} = 94.88\% \pm 0.015$$

8.4 Analysis of the Air Pressure Measurement Entering Cooling Coil

The following readings are air pressure before cooling coil taken by strain-gauge presssure transducer and recorded by data acquisition system. The unit was in Parcel and by the below equations, it is transferred to in - H_2O.

Psi X 6894.757 = P_a

Psi X 27.673 = in - H_2O

Reading	Air Pressure	$X_i - \bar{X}$	$(X_i - \bar{X})^2$
1	2.10 in H_2O	0.03	0.0009
2	2.09	0.02	0.0004
3	2.12	0.05	0.0025
4	2.15	0.08	0.0064
5	2.10	0.03	0.0009
6	2.08	0.01	0.0001
7	2.11	0.04	0.0016
8	2.15	0.08	0.0064
9	2.11	0.04	0.0016
10	2.07	0	0
11	2.12	0.05	0.0025
12	2.11	0.04	0.0016
13	2.08	0.01	0.0001
14	2.03	-0.04	0.0016
15	2.02	-0.05	0.0025
16	2.04	-0.03	0.0009
17	2.08	0.01	0.0001
18	2.03	-0.04	0.0016
19	2.00	-0.07	0.0049
20	2.03	-0.04	0.0016
21	2.07	0	0
22	2.01	-0.06	0.0036
23	2.00	-0.07	0.0049
24	2.04	-0.03	0.0009
25	2.03	-0.04	0.0016
26	2.01	-0.06	0.0036
n=26	$\Sigma\|X_i - \bar{X}\| = 53.78$	$\Sigma\|X_i - \bar{X}\| = 1.02$	$\Sigma(X_i - \bar{X})^2 = 0.0528$

TABLE 20

The mean value is :

$$\bar{X} = \frac{1}{n} \sum_{i=1}^{n} X_i = \frac{1}{26} (53.78) = 2.07 \text{ in. } H_2O$$

And the standard deviation is :-

$$\sigma = \frac{1}{n} \sum_{i=1}^{n} \left[(X_i - \bar{X})^2 \right] = \frac{1}{26} (0.0528)^{\frac{1}{2}} = 0.008 \text{ in. } H_2O$$

Thus, in accordance with the normal probability curve, if are arbitrary select any single reading :

$\bar{X}$	= 2.07	$\pm$	0.008	68.3%
$\bar{X}$	= 2.07	$\pm$	0.016	95 %
$\bar{X}$	= 2.07	$\pm$	0.032	99.7%

REFERENCES

1. Methods of testing forced circulation air cooling and heating coils, ASHRAE STANDARD 33-78.

2. Standard for Forced Circulation and Air Cooling and Heating Coils. ARI Standard 410-77.

3. Aboul Hakin, H. Elmah Dy, "Analytical and Experimental Multi-Row, Finned Tube, Heat Exchanger Performance During Cooling and Dehumidifying Process", Ph.D. Theses, 1975, Page 7, 8.

4. A.S.H.V.E. Transaction, Vol 44, 1938, Page 523.

5. Heating, Piping and Air Conditioning, Feb. 1945, Journal Section, Page 90.

6. Heating, Piping and Air Conditioning, Nov. 1938 to May 1939, Goodman.

7. Theory of moist air heat exchanger, G. Brown, 1954.

8. Transaction of the Royal Institute of Technology Stockholm, M77-1954, G. Brown.

9. James L. Threlkeld. "Thermal Environments Engineering", 1970.

10. R.J. Myers. "The effect of dehumidification on the air side heat transfer coefficient for a finned tube coil", 1967.

11. Engineering Analysis of Experimental Data, ASHRAE STANDARD 41-5-75.

12. Rich, D.G., ASHRAE Research in Heat Transfer, ASHRAE Journal, Vol 7, No. 1, January 1965, Page 105.

13. Ashley, C.M., The Heat Transfer of Evaporating Freon, Refrigerating Engineering, Vol 43, No. 2, Feb. 1942, Page 89.

14. Baker, M., Heat Transfer Rates From Heated Horizontal Tubes to Dichlorodifluromethane, Refrigerating Engineering, Vol 64, No. 1, Jan. 1956, Pages 35 - 37.

15. Worsoe-Schmidt, P., Some Characteristic of Flow Pattern and Heat Transfer of Freon-12 Evaporating in Horizontal Tubes, Journal of Refrigeration, Vol 3, No. 2, March-April 1960, Pages 40-4.

16. Pierre, B., Varmeorergangen vid Kokande Koldmedier; Horisontella Ror, Kyltenknisk Tidskrift, No. 3, March 1957.

Table 21 shows a comparison of the results between the manual and computerized calculations for some of the major parameter in the test.

	Manual Calculation	Computer Calculation
W_1	0.01080	0.01074
W_2	0.00634	0.00640
V_n	12.920	12.937
W_A	123.52	123.35
V_A	219.6	219.3
t_1	79.97	79.98
t_2	47.83	47.84
h_1	31.34	30.98
h_2	18.05	18.41
q_{tu}	97682	92518
q_{su}	57405	57777
q_{t2}	96200	96200
q_s	56970	58927

TABLE 21

COMPARISON OF THE MANUAL AND COMPUTERIZED CALCULATION RESULTS

APPENDIX 2

MAJOR EQUIPMENT SPECIFICATIONS

A. TEST COIL

Type:	Direct Expansion
Tube arrangement:	Staggered
Type of Fin:	Configurated Fin Tube Plate
Fin Collars:	Full
Material:	Aluminum (Intial Temperature H112)
Thickness:	0.0065 in (0.165 mm)
Tube Material:	Copper (annealed and Skin Hardened)
Nominal Diameter:	0.5" (1.27 mm)
Internal Tube Surface:	Smooth
Type of Fin-Tube Bond:	Mechanical Expansion
Direction of Air Flow:	Horizontal
Orientation of Coil Face:	Vertical
Position of Tubes:	Horizontal
Number of Coil Circuits:	10
Number of Rows:	4
Coil Face Area:	22 1/2" x 48" = 7.5 sq.ft. ($0.697 m^2$)
Fin Depth in the Direction of Air Flow:	6 in. (152.4 mm)
Refrigerant Used For Tests:	R-22

B. AIR HANDLING UNIT

Rates Air Volume:	600 c.f.m. (2832 l/s)
Rated Static Pressure:	5 1/2 in. w.g. (1.369 kPa)

Type:	Centrifugal
Air Volume Control:	Outlet Damper
Impeller Diameter:	15 in. (381 mm)

C. HEATING COIL

Face Area:	30 in x 36 in (7.5 sq.ft.), 0.697m^2)
Number of Rows:	6
Nominal Tube Dia.:	2 in (copper), (50.88 m^2)
Fin Material:	Aluminum
Rated Capacity:	120,000 Btu, (35 kw)

D. REFRIGERATION SYSTEM

Rated Capacity:	10 tons (35 kw)
Refrigerant:	R-22
Belt Driven Condenser:	Water Cooled
Capacity Control:	Hot Gas By-Pass

F. HEATING SYSTEM

Boiler:	Electric - Hot water/Steam
Rated Capacity:	60 k.w., 550V, 3 Phase, 60 cycle
Rated Steam Pressure:	
Max. Pressure:	Max. 100 PSIG (689 kPa)
Operating Pressure:	(1034 kPa)
Hot Water: Flow:	20 GPM (126 t/s)
Max. Temp:	225°F (107 °C)

APPENDIX 3

VELOCITY PROFILE BEFORE COOLING COIL

Hole # / depth	1	2	3	4	5	6	7	8	
A	0.52 X 0.05 649	0.71 X 0.05 759	0.75 X 0.05 780	0.75 X 0.05 780	0.55 X 0.05 668	0.60 X 0.05 698	0.58 X 0.05 686	0.51 X 0.05 643	h_v V
B	0.55 X 0.05 663	0.69 X 0.05 748	0.76 X 0.05 785	6.77 X 0.05 790	0.56 X 0.05 674	0.59 X 0.05 692	0.57 X 0.05 680	0.52 X 0.05 649	h_v V
C	0.51 X 0.05 643	0.69 X 0.05 621	0.75 X 0.05 769	0.75 X 0.05 780	0.5 X 0.05 637	0.57 X 0.05 680	0.57 X 0.05 680	0.54 X 0.05 662	h_v V
D	0.49 X 0.05 630	0.67 X 0.05 734	0.7 X 0.05 759	0.70 X 0.05 753	0.47 X 0.05 617	0.54 X 0.05 662	0.56 X 0.05 674	0.53 X 0.05 656	h_v V

TABLE 22

Type of inst: Pitof tube

No.of Nozzle open : 3

1 Pamper opening: Max.

RPM of Fan: 2935

Barometric Pressure: 30.63

$h_s = 3.42$

$T = 33.5^{\circ}C$

$$V = 4000 \sqrt{\frac{30}{B} \times \frac{T}{528} \times \frac{408}{408 + h_s} \times h_v}$$

$V_{av} = 701$ ft/min

$$\% dv = \frac{790 - 617}{790} \times 100 = 21.9\%$$

APPENDIX 4

SUMMARY OF COMPUTER INPUT AND OUTPUT DATA

Test Number

ITEM	I	II	III	IV	V	VI
P_b	30.8	30.8	30.8	30.8	30.8	30.8
t_3	80.2	80.2	80.2	80.2	80.2	80.2
t'_3	67.1	67.1	67.1	67.1	67.1	67.1
t_4	47.2	47.9	48.8	50	51.6	53.4
t'_4	46.2	47	47.9	49.1	50.8	52.4
t_5	75.6	75.6	75.6	75.6	75.6	75.6
ΔP_a	0.37	0.38	0.4	0.42	0.48	0.56
P_{a1}	0.35	0.53	0.75	1.02	1.42	1.93
ΔP_N	0.22	0.33	0.47	0.67	0.95	1.35
P_N	0.63	0.51	0.41	0.29	0.17	0.03
t_N	47.2	47.9	48.8	50	51.6	53.4
t'_{r2}	42.3	43.1	43.2	43.7	44.6	46.7
P_{r2}	54.2	54.5	55.4	56.3	57.8	60.8
ΔP_r	16.3	20.4	24.4	28.7	32.6	36.3
ΔP_{rc}	8.2	10.1	12.2	14.4	16.3	18.2
h_{r1}	36.1	36	36	36	36	36
h_{r2}	109.5	110.3	110.3	100.6	111	111.6
w_r	1100	1300	1460	1620	1770	1915
t_{w1}	70.1	70.1	70.1	70.1	70.1	70.1
t_{w2}	85.2	85.2	85.2	85.2	85.2	85.2
M	1443	1693	1587	2120	2327	2526
Z	30	30	30	30	30	30
Pc1	203.0	203.0	203.0	203.0	203.0	203.0
t_a	76.5	76.5	76.5	76.5	76.5	76.5
K_c	0.1	0.1	0.1	0.1	0.1	0.1
q_c	14.2	14.2	14.2	14.2	14.2	14.2
h_{c1}	124.4	124.4	124.8	125.2	125.2	126.0
h_{c2}	37.0	37.0	37.0	37.0	37.0	37.0
A_N	.698	.698	.698	.698	.698	.698
C_N	.99	.99	.99	.99	.99	.99
K_{31}	9.5	9.5	9.5	9.5	9.5	9.5
K_{24}	4.0	4.0	4.0	4.0	4.0	4.0
AF	7.5	7.5	7.5	7.5	7.5	7.5
RT	22	22	22	22	22	22

Table 23- Summary of Input Data

Note: Experimental data reduction was performed using the computerized data reduction programme recommended by the ASHRAE Standard

Test Number

ITEM	I	II	III	IV	V	VI
W1 (1,2)	.01075	.01074	.01074	.01073	.01072	.01070
W2 (1,2)	.00618	.00640	.00663	.00694	.00743	.00785
VN (1,2)	12.914	12.937	12.964	13.002	13.053	13.208
WA (1,2)	101.01	123.35	146.80	174.66	207.11	245.76
VA (1,2)	179.6	219.3	261.0	310.5	368.2	436.9
T1 (1,2)	79.97	79.98	79.98	79.98	79.99	79.99
H1 (1,2)	30.98	30.98	30.97	30.96	30.95	30.93
T2 (1,2)	47.12	47.84	48.75	49.96	51.57	53.38
H2 (1,2)	18.00	18.41	18.88	19.51	20.43	21.32
T1-T2	32.85	32.14	31.23	30.02	28.42	26.61
QTA (1,2)	78280	92518	105933	119313	129923	140862
QSA (1,2)	48337	57777	66846	76503	85945	95583
QTZ (1)	80.850	96.200	108478	120852	132750	144774
QTZ (2)	81,374	96.118	109426	121312	133852	146520
QTZ (AV)	81,112	96,159	108.952	121,082	133,301	145,647
QT (1)	79565	94359	107205	120082	131336	142818
QT (2)	79827	94318	107679	120312	131887	143691
QT (AV)	79,696	94,339	107,442	120,197	131,612	143,255
QS (1)	49131	58927	67649	76996	86880	96910
QS (2)	49293	58901	67948	77144	87245	97503
QS (AV)	49,212	58,914	67,799	77,070	87,063	97,207
HBT (1)	-3.23	-3.90	-2.37	-1.28	-2.15	-2.74
HBT (2)	-3.88	-3.82	-3.24	-1.66	-.298	-3.94
HBS (1,2)	0	0	0	0	0	0
PR1 (1,2)	85.62	89.72	94.92	100.12	105.62	112.22
PRC2 (1,2)	77.42	79.72	82.72	85.72	89.32	94.02
DPRH (1,2)	8.100	10.100	12.200	14.300	16.300	18.100
TR1 (1,2)	41.64	44.34	47.65	50.82	54.05	57.77
TR2 (1,2)	29.81	30.05	30.75	31.45	32.67	34.83
TRSH2 (1,2)	12.99	12.95	12.45	12.25	11.93	11.87
DPS (1,2)	.383	.394	.414	.434	.496	.578

(1) Ref. Liquid flow Method
(2) Condenser Water Method

Table 24- Summary of Output Data

```
 ENTER DATA- RT, AF, K24, K31, CN AND AN.
   CODING -
     RT = REFRIGERANT TYPE NUMBER, UNIT '12' OR '22'.
     AF = TEST COIL FACE AREA, UNIT SQ.FT.
     K24 = AIR MIXING CHAMBER HEAT LEAK, UNIT BTU/(HR)(F).
     K31 = AIR INTAKE CHAMBER HEAT LEAK, UNIT BTU/(HR)(F).
     CN = AIR NOZZLE COEFFICIENT.
     AN = AIR NOZZLE(S) AREA, UNIT SQ.FT.
? 22,7.5,4,9.5,.99,.698

 ENTER DATA- PB, T3, TP3, T4, TP4 AND T5.
   CODING -
     PB = BAROMETRIC PRESSURE DURING TEST, UNIT HG ABS.
     T3 = D.B. ENT. INTAKE CHAMBER, UNIT F.
     TP3 = W.B. ENT. INTAKE CHAMBER, UNIT F.
     T4 = D.B. OUT. MIXING CHAMBER, UNIT F.
     TP4 = W.B. OUT. MIXING CHAMBER, UNIT F.
     T5 = AVERAGE D.B. AROUND TEST CHAMBER, UNIT F.
? 30.8,80,67,47.2,46.2,75.6

 ENTER DATA- DPA, PA1, DPN, PN, TN AND TPR2.
   CODING -
     DPA = AIR SIDE PRESS DROP THRU TEST COIL, UNIT HG.
     PA1 = AIR STATIC AT TEST COIL INLET, UNIT HG.
     DPN = STATIC PRESS DIFF. ACROSS NOZZLES, UNIT HG.
     PN = STATIC PRESS AT NOZZLE THROAT, UNIT HG.
     TN = D.B. ENT. AIR NOZZLE(S), UNIT F.
     TPR2 = SUPER HEATED REF. OUT SUCT. HDR., UNIT F.
? .37,.35,.22,.63,47.2,42.8

 ENTER DATA- PR2, DPR, DPRC, HR1 AND HR2.
   CODING -
     PR2 = REFRIGERANT VAPOR PRESS OUT. COIL SUCT. HDR., UNIT PSIG.
     DPR = REF. PRESS DROP THRU COIL & HDR., UNIT PSI.
     DPRC = REFRIGERANT PRESS DROP THRU COIL CIRCUIT, UNIT PSI.
     HR1 = ENTHALPY OF REF. ENT. COIL, UNIT BTU/LB.
     HR2 = ENTHALPY OF REGRIGERANT VAPOR OUT, COIL, UNIT BTU/LB.
? 54.2,16.3,8.2,36,109.5,

 ENTER DATA- WRF, TW1, TW2, M AND Z.
   CODING -
     WRF = REFRIGERANT FLOW THRU FLOW METER.
     TW1 = ENT. WATER(FLUID) TEMP., UNIT F.
     TW2 = LEAVING WATER(FLUID) TEMP., UNIT F.
     M = WEIGHT OF WATER(FLUID) COLLECTED, UNIT LBS.
     Z = TIME REQUIRED TO COLLECT WATER(FLUID), UNIT MINUTE.
? 1145,70,85,2270,20

 ENTER DATA- PC1, TA, KC, QCOM, HC1 AND HC2.
   CODING -
     PC1 = REF. VAPOR PRESS ENT. COND., UNIT PSIG.
     TA = AVERAGE SURROUND REFRIGERANT COND., UNIT F.
     KC = COND. INSULATION COEFF., UNIT BTU/(HR)(F).
     QCOM = CAP. OF CALB. COMP., UNIT BTU/HR.
     HC1 = ENTHALPY OF REFRIGERANT ENT. COND. OR COMP., UNIT BTU/LB.
     HC2 = ENTHALPY OF REFRIGERANT OUT COND. OR COMP., UNIT BTU/LB.
? 203,76.5,.1,14.2,125,37
```

SAMPLE OF INPUT DATA

REFRIGERANT COIL TRIAL # 1

W1 = .01075	W2 = .00618	VN = 12.914	WA = 101.01
VA = 179.6	T1 = 79.97	H1 = 30.98	T2 = 47.12
H2 = 18.00	QTA = 78280.	QSA = 48337.	QTZ = 85321.
QT = 81800.	QS = 50511.	HBT = -8.61	HBS = 0.00
PR1 = 85.62	PRC2 = 77.42	DPRH = 8.100	TR1 = 41.64
TR2 = 29.81	TRSH2 = 12.99	DPS = .383	

CODING -

W1 = ENT. HUMIDITY RATIO, UNIT #WV/LB DA.
W2 = LEAVING HUMIDITY RATIO, UNIT #WV/LB DA.
VN = SPEC. VOL. OF AIR VAPOR MIX AT STD. PB, UNIT CU.FT/LB DA.
WA = DRY AIR FLOW RATE, UNIT #DA/MIN.
VA = STD. AIR FACE VEL., UNIT FT/MIN.
T1 = DS ENT. COIL, UNIT F.
H1 = ENTHAPY OF AIR ENTERING COIL.
T2 = D.B. LEAVING COIL, UNIT F.
H2 = ENTHALPY OF AIR LEAVING COIL.
QTA = TOTAL AIR SIDE HEAT CAPACITY, UNIT BTU/HR.
QSA = SENSIBLE AIR SIDE HEAT CAPACITY, UNIT BTU/HR.
QTZ = TOTAL FLUID SIDE HEAT CAPACITY, UNIT BTU/HR.
QT = AVERAGE TOTAL HEAT CAPACITY, UNIT BTU/HR.
QS = AVERAGE SENSIBLE HEAT CAPACITY, UNIT BTU/HR.
HBT = HEAT BALANCE TOTAL, UNIT %.
HBS = HEAT BALANCE SENSIBLE, UNIT %.
PR1 = ABS. REF. PRESS AT COIL INLET, UNIT PSIA.
PRC2 = ABS. REF. PRESS OUT COIL CIRCUIT, UNIT PSIA.
DPRH = REF. PRESS DROP ACROSS SUCT. HDR., UNIT PSI.
TR1 = SAT. REF. AT COIL INLET, UNIT F.
TR2 = SAT. REF. AT COIL OUTLET.
TRSH2 = REF. VAPOR S.H. AT COIL OUT.
DPS = STD. AIR PRESS DROP, UNIT HG.

TABLE 25 OUTPUT FOR TEST NO. 1

REFRIGERANT COIL TRIAL # 1

W1 = .01074	W2 = .00640	VN = 12.937	WA = 123.35
VA = 219.3	T1 = 79.98	H1 = 30.98	T2 = 47.84
H2 = 18.41	QTA = 92518.	QSA = 57777.	QTZ = 97253.
QT = 94886.	QS = 59256.	HBT = -4.99	HBS = 0.00
PR1 = 89.72	PRC2 = 79.72	DPRH = 10.100	TR1 = 44.34
TR2 = 30.05	TRSH2 = 12.95	DPS = .394	

TABLE 26. OUTPUT FOR TEST NO. 2

REFRIGERANT COIL TRIAL # 1

W1 = .01074	W2 = .00663	VN = 12.964	WA = 146.80
VA = 261.0	T1 = 79.98	H1 = 30.97	T2 = 48.75
H2 = 18.88	QTA = 105933.	QSA = 66846.	QTZ = 109426.
QT = 107679.	QS = 67948.	HBT = -3.24	HBS = 0.00
PR1 = 94.92	PRC2 = 82.72	DPRH = 12.200	TR1 = 47.65
TR2 = 30.75	TRSH2 = 12.45	DPS = .414	

TABLE 27. OUTPUT FOR TEST NO. 3

REFRIGERANT COIL TRIAL # 1

W1 = .01073	W2 = .00694	VN = 13.002	WA = 174.66
VA = 310.5	T1 = 79.98	H1 = 30.96	T2 = 49.96
H2 = 19.51	QTA = 119313.	QSA = 76503.	QTZ = 121312.
QT = 120312.	QS = 77144.	HBT = -1.66	HBS = 0.00
PR1 = 100.12	PRC2 = 85.72	DPRH = 14.300	TR1 = 50.82
TR2 = 31.45	TRSH2 = 12.25	DPS = .434	

TABLE 28. OUTPUT FOR TEST NO. 4

REFRIGERANT COIL TRIAL # 1

W1 = .01072	W2 = .00743	VN = 13.053	WA = 207.11
VA = 368.2	T1 = 79.99	H1 = 30.95	T2 = 51.57
H2 = 20.43	QTA = 129923.	QSA = 85945.	QTZ = 130400.
QT = 130161.	QS = 86103.	HBT = -.37	HBS = 0.00
PR1 = 105.62	PRC2 = 89.32	DPRH = 16.300	TR1 = 54.05
TR2 = 32.67	TRSH2 = 11.93	DPS = .496	

TABLE 29. OUTPUT FOR TEST NO. 5

REFRIGERANT COIL TRIAL # 1

W1 = .01070	W2 = .00785	VN = 13.108	WA = 245.76
VA = 436.9	T1 = 79.99	H1 = 30.93	T2 = 53.38
H2 = 21.32	QTA = 140862.	QSA = 95583.	QTZ = 146520.
QT = 143691.	QS = 97503.	HBT = -3.94	HBS = 0.00
PR1 = 112.22	PRC2 = 94.02	DPRH = 18.100	TR1 = 57.77
TR2 = 34.83	TRSH2 = 11.87	DPS = .578	

TABLE 30. OUTPUT FOR TEST NO. 6

APPENDIX 5

PHOTOGRAPHS OF THE INSTALLATION AND EQUIPMENT

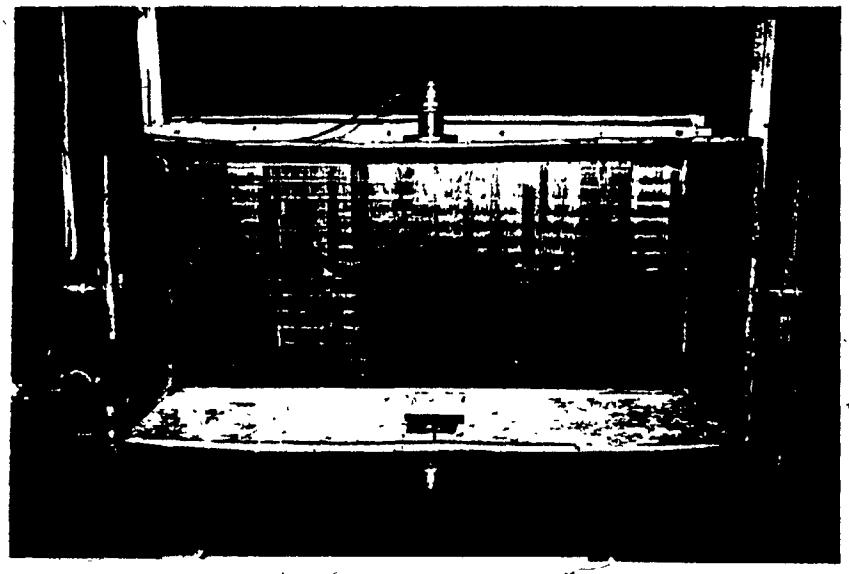

The Direct Expansion Test Coil

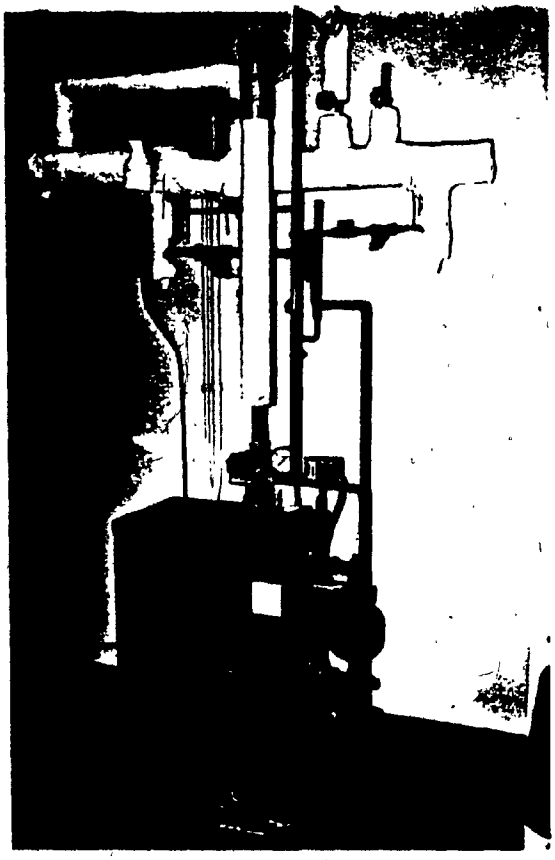

Electric Steam Boiler

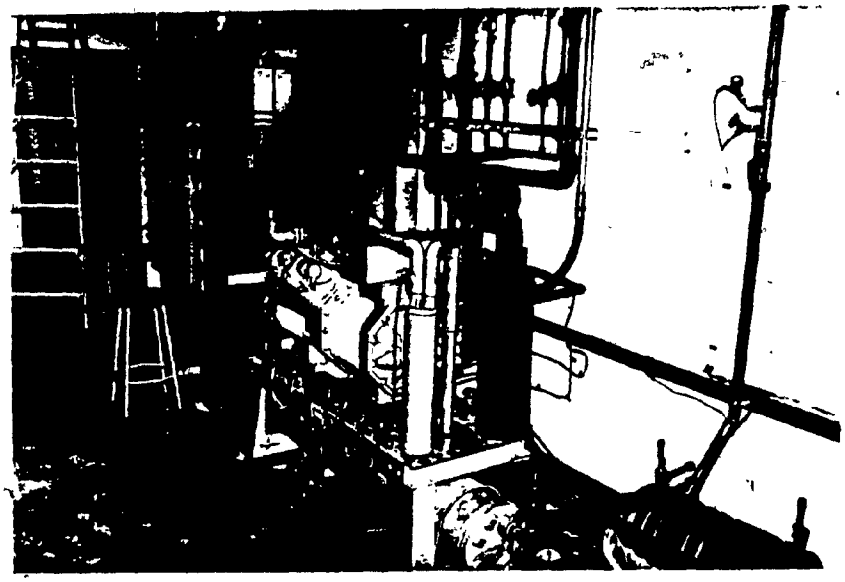

The Refrigeration System

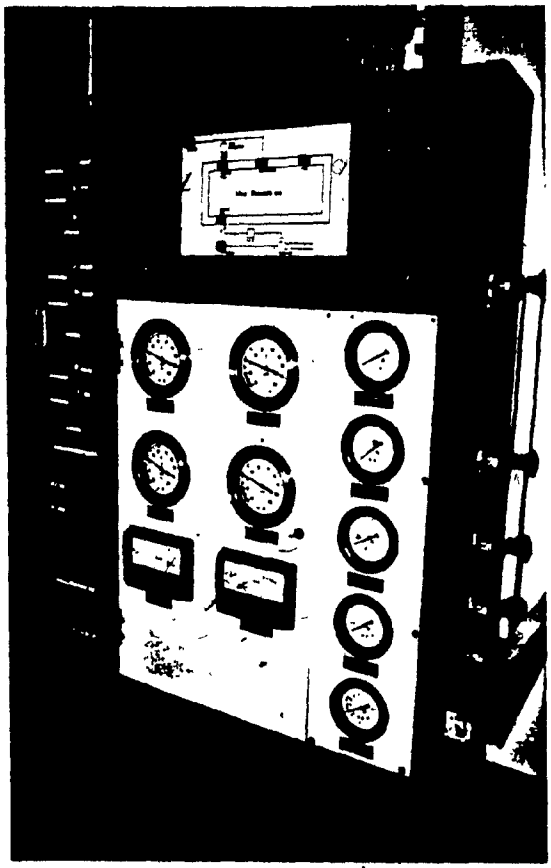

Control Panel

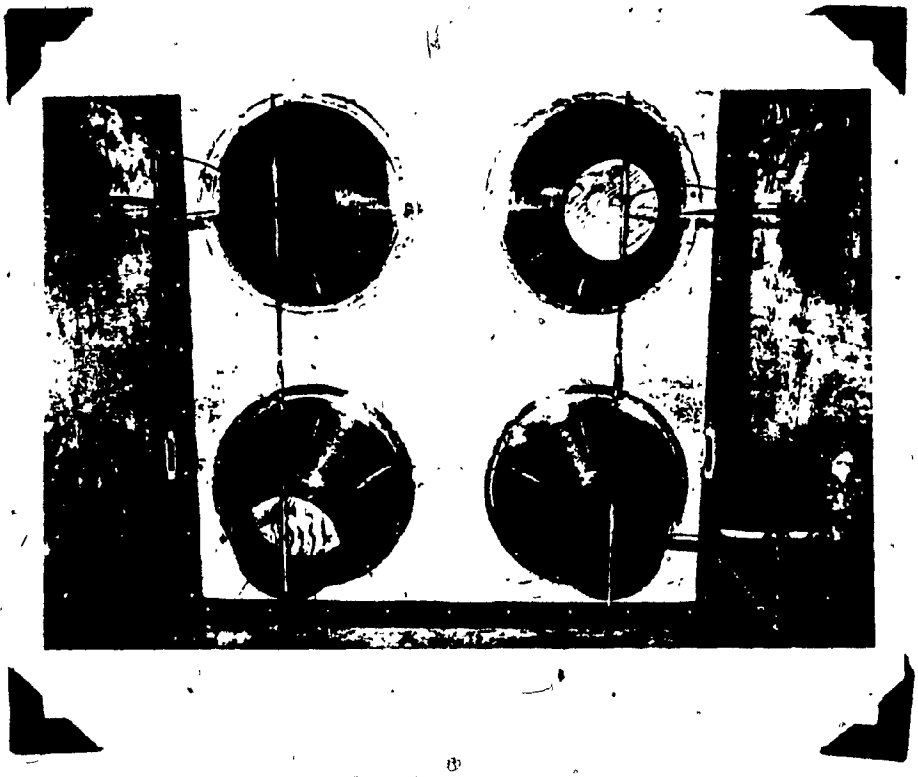

THe Nozzle Plate

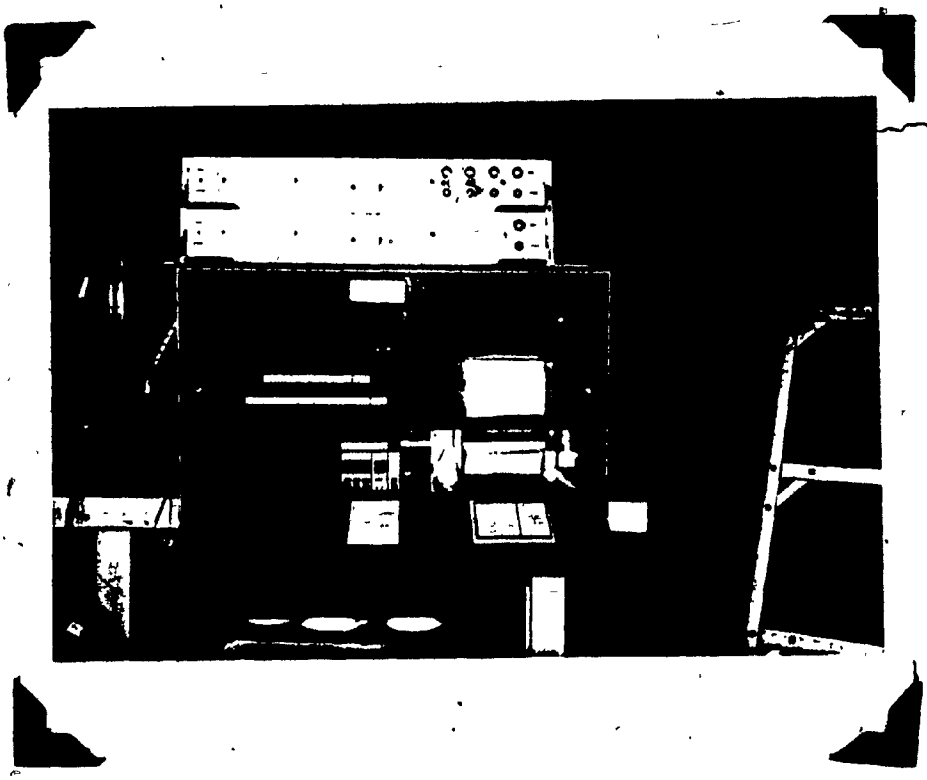

Data Acquisition System